

# Accepted Manuscript

Structure-based design and synthesis of 2,4-diaminopyrimidines as EGFR L858R/T790M selective inhibitors for NSCLC

Lingfeng Chen, Weitao Fu, Chen Feng, Rong Qu, Linjiang Tong, Lulu Zheng, Bo Fang, Yinda Qiu, Jie Hu, Yuepiao Cai, Jianpeng Feng, Hua Xie, Jian Ding, Zhiguo Liu, Guang Liang

PII: S0223-5234(17)30673-6

DOI: [10.1016/j.ejmech.2017.08.061](https://doi.org/10.1016/j.ejmech.2017.08.061)

Reference: EJMECH 9705

To appear in: *European Journal of Medicinal Chemistry*

Received Date: 6 July 2017

Revised Date: 25 August 2017

Accepted Date: 28 August 2017

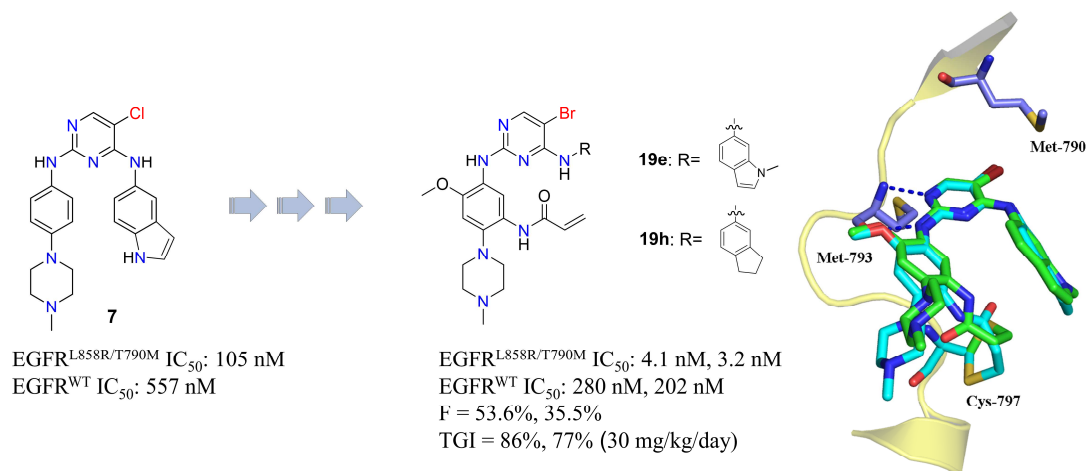
Please cite this article as: L. Chen, W. Fu, C. Feng, R. Qu, L. Tong, L. Zheng, B. Fang, Y. Qiu, J. Hu, Y. Cai, J. Feng, H. Xie, J. Ding, Z. Liu, G. Liang, Structure-based design and synthesis of 2,4-diaminopyrimidines as EGFR L858R/T790M selective inhibitors for NSCLC, *European Journal of Medicinal Chemistry* (2017), doi: 10.1016/j.ejmech.2017.08.061.

This is a PDF file of an unedited manuscript that has been accepted for publication. As a service to our customers we are providing this early version of the manuscript. The manuscript will undergo copyediting, typesetting, and review of the resulting proof before it is published in its final form. Please note that during the production process errors may be discovered which could affect the content, and all legal disclaimers that apply to the journal pertain.



## Graphical Abstract

Structure-based design and synthesis of 2,4-diaminopyrimidines as EGFR L858R/T790M selective inhibitors for NSCLC



**Keywords:** epidermal growth factor receptor; tyrosine kinase inhibitors; non-small cell lung cancer; T790M; mutant-selective.

Structure-based design and synthesis of 2,4-diaminopyrimidines as EGFR L858R/T790M selective inhibitors for NSCLC

Lingfeng Chen <sup>a,b,1</sup>, Weitao Fu <sup>a,1</sup>, Chen Feng <sup>a,1</sup>, Rong Qu <sup>c</sup>, Linjiang Tong <sup>c</sup>,  
Lulu Zheng <sup>a</sup>, Bo Fang <sup>a</sup>, Yinda Qiu <sup>a</sup>, Jie Hu <sup>a</sup>, Yuepiao Cai <sup>a</sup>, Jianpeng Feng <sup>a</sup>,  
Hua Xie <sup>c</sup>, Jian Ding <sup>c,\*\*\*</sup>, Zhiguo Liu <sup>a,\*\*</sup>, Guang Liang <sup>a,b,\*</sup>

<sup>a</sup> School of Chemical Engineering, Nanjing University of Science and Technology, Nanjing, Jiangsu, 210094, China

<sup>b</sup> Chemical Biology Research Center at School of Pharmaceutical Sciences, Wenzhou Medical University, Wenzhou, Zhejiang 325035, China

<sup>c</sup> Division of Anti-Tumor Pharmacology, State Key Laboratory of Drug Research, Shanghai Institute of Materia Medica, Chinese Academy of Sciences, Shanghai, 201203, China

<sup>1</sup> These authors contributed equally to this work.

\*Corresponding authors:

Prof. Guang Liang

Chemical Biology Research Center,

School of Pharmaceutical Sciences,

Wenzhou Medical University,

Wenzhou, Zhejiang, 325035, P. R. China.

Tel./fax: +86 577 86699396.

E-mail addresses: wzmcliangguang@163.com (G. Liang).

and

Jian Ding<sup>\*\*\*</sup>, Ph.D, Professor, E-mail: jding@simm.ac.cn

Zhiguo Liu<sup>\*\*</sup>, Ph.D, Associate Professor, E-mail: lzgcnu@163.com

**Abstract**

Mutated epidermal growth factor receptor (EGFR) is a major driver of non-small cell lung cancer (NSCLC). The EGFR<sup>T790M</sup> secondary mutation has become a leading cause of clinically-acquired resistance to gefitinib and erlotinib. Herein, we present a structure-based design approach to increase the potency and selectivity of the previously reported reversible EGFR inhibitor **7**, at the kinase and cellular levels. Three-step structure-activity relationship exploration led to promising compounds **19e** and **19h** with unique chemical structure and binding mode from the other third-generation tyrosine kinase inhibitors. In a human NSCLC xenograft model, **19e** and **19h** exhibited dose-dependent tumor growth suppression without toxicity. These selective inhibitors are promising drug candidates for EGFR<sup>T790M</sup>-driven NSCLC.

**Keywords:** epidermal growth factor receptor; tyrosine kinase inhibitors; non-small cell lung cancer; T790M; mutant-selective.

## 1. Introduction

Lung cancer remains one of the most common and deadly cancers worldwide, with approximately 1.8 million new cases diagnosed annually and a 5-year survival rate less than 20% [1]. Almost 85% of all lung cancers are identified as non-small cell lung cancer (NSCLC) [2,3]. The epidermal growth factor receptor (EGFR) protein has been identified as a valuable therapeutic target for NSCLC. EGFR plays an indispensable role in cancer cell proliferation, survival, migration, adhesion and differentiation [4,5]. Hence, inhibition of activated EGFR using small-molecule kinase inhibitors can suppress the signaling pathway, reduce the oncogenic drive, and result in the inhibition of tumor growth.

The first generation of EGFR inhibitors (gefitinib and erlotinib) has achieved remarkable benefits in patients carrying “sensitizing mutations” such as L858R and exon-19 deletions. However, efficacy of these inhibitors was limited because of the acquired Thr790Met (T790M) point mutation in exon 20 at the “gatekeeper” position of EGFR kinase domain [6,7]. The bulkier methionine residue is thought to sterically obstruct the binding of the reversible first generation inhibitors, thus disrupting the formation of a crucial hydrogen bond between the inhibitor and the EGFR T790M site [8-10]. In addition, the T790M mutation is believed to increase the affinity of the kinase for ATP [11]. Subsequently, a number of second-generation irreversible inhibitors such as afatinib [12], neratinib [13], and dacomitinib [14] were developed, based on the anilinoquinazoline scaffold of gefitinib. These inhibitors contain an electrophilic Michael addition receptor moiety that can covalently bind the conserved

cysteine residue (Cys797) of EGFR to facilitate the occupation of the EGFR ATP binding site and overcome the resistance caused by the T790M [15]. However, second-generation inhibitors not only have increased activity against the sensitizing and resistant mutations, but also against wild-type (WT) EGFR. Therefore, their clinical efficacy has been limited due to dose-limiting WT EGFR-driven toxicities including skin rash and diarrhea [16]. Therefore, it is highly desirable to develop selective inhibitors targeting EGFR<sup>T790M</sup>.

With the aim to identify inhibitors selective for the EGFR<sup>T790M</sup> while sparing EGFR<sup>WT</sup>, Zhou and co-workers [17] discovered WZ4002 (**1**, Figure 1) by. The co-crystal structure of the EGFR<sup>T790M</sup> kinase domain in complex with **1** showed that a “U-shaped” configuration of a pyrimidine core in the structure of **1** is favorable for binding. Since that published report, a great number of third generation inhibitors were designed and synthesized as selective inhibitors of T790M-containing EGFR. Compound **2** (CO-1686/rociletinib) reached phase II clinical trials in NSCLC patients with EGFR T790M-positive mutation (NCT02147990) [18]. However, the development of **2** has been discontinued due to its inhibition of the insulin-like growth factor 1 receptor (IGF1R) and the insulin receptor (INSR) [19, 20]. Recently, the U. S. Food and Drug Administration granted accelerated approval to **3** (AZD9291/osimertinib) for the treatment of patients harboring EGFR<sup>T790M</sup> mutation [21, 22]. Michellys *et al* [23] reported the discovery of **4** (EGF816, nazartinib), a potent covalent mutant-selective EGFR inhibitor with a unique structural motif, which is currently being evaluated in a number of clinical trials for the treatment of NSCLC

(NCT02335944, NCT02323126). In addition, Ding *et al* [24-26] and other groups [27-28] explored the fusion of heterocycles ring onto the scaffold of WZ4002 and designed numerous derivatives such as **5** and **6** as potential inhibitors through conformational constraints strategies.

In this study, we describe the design and optimization of 2,4-diamino-pyrimidine derivatives as novel EGFR<sup>L858R/T790M</sup> inhibitors with improved selectivity profiles over EGFR<sup>WT</sup> based on the lead compound **7**, previously discovered by our group [29]. A three-step structure-based modification strategy led to two potent molecules, **19e** and **19h**, representing promising candidates with a different chemical scaffold and binding mode that target EGFR<sup>L858R/T790M</sup> for the treatment of NSCLC.

*Please insert Figure 1 here*

## 2. Results and Discussion

### 2.1. Chemistry

The synthetic route of **14a-14h**, **15a-15j** is outlined in Scheme 1. Reaction of the commercially available 2,4-dichloro-5-substitued-pyrimidines (**8a-8g**) or 4,6-dichloro-1*H*-pyrazolo[3,4-*d*]pyrimidine (**8h**) with indol-5-amine produced intermediates **10a-10h** [18]. Commercially available 4-fluoronitrobenzene reacted with 1-methylpiperazine in the presence of K<sub>2</sub>CO<sub>3</sub> to provide the intermediate **12**. The catalytic hydrogenation of the nitro-group with Pd/C provided the desired aniline **13** in high yield [30]. Nucleophilic aromatic substitution of the 2-chloro position in

**10a-10g** with **13** in 2-butanol catalyzed by trifluoroacetic acid at 100°C yielded compounds **14a-14g**, while intermediate **10h** reacted with **13** in 2-pentanol with *p*-TSA yielding **14h**. Similarly, 5-bromo-2,4-dichloropyrimidine (**8g**) reacted with various amines (**9a-9j**), yielding intermediates **11a-11j**, and the subsequent substitution by **13** provided target compounds **15a-15j**. The preparation of amines **9d** and **9e** is shown in Supporting Information.

The general strategy to install the Michael receptor warhead in compounds **15a**, **15e** and **15f** is shown in Scheme 2. For compounds where  $R^3 = H$ , commercial aniline **20a** was used. Where  $R^3 =$  methoxy group, 4-fluoro-2-methoxy-5-nitroaniline (**20b**) was synthesized by nitration of 2-methoxy-4-fluoro-aniline. Aniline addition of **20a** or **20b** to 2-chloropyrimidines **11a**, **11e** and **11f** was achieved by acid-catalyzed  $S_NAr$  reaction in 2-pentanol with *p*-TSA, yielding intermediates **16a-16f**. 1-methylpiperazine or  $N^1,N^1,N^2$ -trimethylethane-1,2-diamine substitution of the fluorine by  $S_NAr$  proceeded with excess of the two amines by heating, providing **17a-17h** in good yield [10]. Subsequent reduction of the nitro group produced the corresponding amines **18a-18h**, which were reacted with acryloyl chloride under carefully monitored conditions in the presence of DIPEA to minimize bis-acryloylated side products, yielding target compounds **19a-19h**. The details of a similar synthesis of target compound **19i** ( $R^1=H$ ) is shown in Supporting Information.

Please insert *Scheme 1* and *Scheme 2* here



## 2.2. Binding mode analysis of lead compound **7**

Based on the structure of **1**, our group previously transferred its phenylacrylamide moiety into a fused heterocyclic ring or replaced by aniline. Among the intermediates generated, a representative compound **7** (Figure 2A), containing an indole headgroup, displays an  $IC_{50}$  of 0.10  $\mu\text{M}$  against the double mutant EGFR (EGFR<sup>L858R/T790M</sup>) and about 5-fold higher selectivity over wild-type EGFR [29]. Therefore, we conducted molecular modeling studies using the crystal structure of EGFR<sup>T790M</sup> and EGFR<sup>WT</sup> (3IKA [17] and 4WKQ) to guide the structural optimization based on **7**. As shown in Figure 2B-C, the 2-aminopyrimidine core of **7** formed two hydrogen bonds with the hinge residue Met793, which showed similar binding modes with the crystal structure of compound **1**. The chlorine substituent at 5-position was directed towards the methionine gatekeeper at 3.2 Å to achieve van der Waals interactions. However, in EGFR<sup>WT</sup> (Figure 2D), the bulkier methionine residue at position 790 was replaced by a smaller and more polar threonine residue. Therefore, hydrophobic interaction between the gatekeeper residue and the chlorine substituent was reduced, leading to lower binding affinity. The 4-methylpiperazin group of **7** was oriented towards the solvent region of the ATP pocket. Interestingly, the indole substituent of **7** entered the hydrophobic pocket close to the kinase hinge and formed a hydrogen bond with the Asn-842 residue. Given these results, we extensively modified the 2,4-diaminopyrimidine scaffold and further explored a systematic structure–activity relationship.

Please insert **Figure 2** here

### 2.3. Explore 5-position substitution directly towards the methionine at 790

Since our modeling predicted the 5-position of **7** was adjacent to the gatekeeper Met-790, we hypothesized that modification of this position may bring about interesting effects on the potency and selectivity of compounds. Thus, analogs of **14a-14h** with chlorine replaced by different substitutions at R<sup>1</sup> were synthesized (Table 1). When the chlorine group was removed from the 5-position (**14a**), the inhibitory effect against EGFR<sup>L858R/T790M</sup> was decreased by approximately 5-fold. On the other hand, the potency against EGFR<sup>WT</sup> improved by 10-fold, indicating the importance of 5-position substitution to maintain the potency and selectivity against EGFR<sup>L858R/T790M</sup>. Introducing a strong electron-withdrawing group such as the trifluoromethyl (**14b**) and nitro (**14c**) groups decreased the potency against EGFR<sup>L858R/T790M</sup> by 5-20 fold. Analogs incorporating an electron-donating group such as methoxy (**14d**) and methyl groups (**14e**) also showed slightly weaker binding against double-mutant EGFR kinase. Among all of the halogen substitution analogs, including **7** (chlorine), **14f** (fluorine) and **14g** (bromine), **14g** showed the most potent inhibitory activity against EGFR<sup>T790M</sup> and EGFR<sup>L858R/T790M</sup> (IC<sub>50</sub> values of 53 and 35 nM, respectively). In addition, **14g** showed almost no inhibitory activity against EGFR<sup>WT</sup> (IC<sub>50</sub> values >1000 nM). Likely, the bromine group of **14g** yielded a suitable size that could form strong van der Waals interaction with the thioether of the methionine at position 790 of EGFR, leading to high selectivity. As the T790M

mutation changes the amino acid residue from a polar threonine to a nonpolar methionine, we also designed a pyrazolo[3,4-*d*]pyrimidine core (**14h**) to increase the hydrophobic interactions between the compound and the Met790 side chain. Unfortunately, the inhibitory activity of **14h** against EGFR<sup>WT</sup> increased over 4-fold compared to **7** with IC<sub>50</sub> values of 127 nM, showing the opposite effect with pyrrolo[2,3-*d*]pyrimidin analogs (PF-06459988 [31] and PF-06747775 [32]) that was recently reported by Pfizer.

*Please insert **Table 1** here*

#### 2.4. Modifications of the right-hand side chain

Taking compound **14g** as our new lead compound, we further investigated the SAR of the R<sup>2</sup> at the hydrophobic pocket of EGFR with other aromatic heterocycles such as indazole, indolin, dihydro-indene, quinoline, and quinoxaline to determine the inhibitory activity and selectivity against double-mutant EGFR kinase. Replacement of indol-5-yl (**14g**) with indol-6-yl (**15a**) and 1-methyl-indole-6-yl (**15e**) slightly increased the activity against EGFR<sup>L858R/T790M</sup>, producing IC<sub>50</sub> values of 19 and 21 nM and more than 60-fold greater selectivity over wild-type EGFR. The introduction of indazol-5-yl (**15b**) and indazol-6-yl (**15c**) barely affected the inhibitory potency against EGFR<sup>L858R/T790M</sup>. However, similar to **15a**, the decreased selectivity of **15b** suggested that 6-position substituted benzoheterocycle might be more favored than the 5-position substituted groups to increase selectivity over wild-type EGFR.

Although the substitution with bulkier 3-fluorobenzyl group (**15d**) decreased selectivity, it maintained activity against EGFR<sup>L858R/T790M</sup>, further validating the predicted binding mode and suggesting that large size moiety at R<sup>2</sup> was tolerated at this hydrophobic region. Interestingly, compound **15f** with 2,3-dihydro-inden substitution maintained potency against double-mutant EGFR kinase, and showed excellent selectivity for the double mutant over wild-type compared to **14g** (194- vs 23-fold). Further modifications with acetyl indolin (**15g-h**) and the six-membered heterocyclic group (**15i-j**) led to complete loss in activity.

*Please insert Table 2 here*

## 2.5. Structure-based design targeting Cys-797

### 2.5.1. Binding mode study of new lead compounds **15a**, **15e**, **15f**

Although these reversible inhibitors (**15a**, **15e**, **15f** with IC<sub>50</sub> values of 19, 21, and 35 nM, respectively) were promising in kinase assays, we observed a 50-fold drop-off in activity when tested in cellular assays (data not shown). This was likely due to high ATP concentrations in the cellular environment [10,11]. However, covalent kinase inhibitors for therapeutic treatments can completely circumvent the high cellular ATP levels and display prolonged on-target residence times [19,33]. Hence, we converted these double-mutant selective compounds into irreversible inhibitors to overcome the loss of activity while maintaining their intrinsic selectivity over the wild-type kinase. The predicted binding mode of compounds **15a**, **15e**, **15f**

was further modeled (Figure 3). Based on their binding mode, we designed compounds incorporated with reactive substituents such as acrylamide targeting Cys-797 to form a covalent bond. We observed that the meta-position of the pyrimidine 2-aniline might be the most ideal with distances of 6.6, 6.4, and 6.1 Å, respectively.

*Please insert Figure 3 here*

#### 2.5.2. Structure-activity relationship studies of irreversible compounds **19a-19i**

Compounds **19a-19i** were synthesized and their IC<sub>50</sub> values determined (Table 3) for validation studies. Additionally, the significance of the ortho-methoxy group at R<sup>3</sup> and the para-4-methylpiperazinyl group at R<sup>4</sup> was investigated. The corresponding irreversible target compounds of **15a**, **15e** and **15f** were first synthesized and named **19b**, **19d** and **19g**, respectively. As expected, all of the compounds showed improved cellular activity in the NCI-H1975 cell line (harboring EGFR<sup>L858R/T790M</sup>) with IC<sub>50</sub> value of less than 0.5 μM; however, selectivity against the double-mutant kinase decreased by approximately 5–11 fold. When the 1-(4-methylpiperazinyl) group of **19b** and **19g** was replaced by *N,N,N'*-trimethylethylenediamine (**19a**, **19f**), the potencies against EGFR<sup>WT</sup> and EGFR<sup>L858R/T790M</sup> kinases both increased approximately 17-80 fold, but led to dramatic loss of selectivity. Similar to the reported data [10,17], the introduction of methoxy group at R<sup>3</sup> (**19c**, **19e** and **19h**) based on **19b**, **19d** and **19g** significantly enhanced the activity and selectivity for EGFR<sup>L858R/T790M</sup> (IC<sub>50</sub> = 2.7,

4.1 and 3.2 nM). Particularly, **19e** and **19h** exhibited 68- and 63-fold increase in selectivity for EGFR<sup>L858R/T790M</sup> kinase, which was similar to that of **3**. In addition, **19e** and **19h** displayed low inhibition of wild-type EGFR-expressing cell line A431 (IC<sub>50</sub> = 1.69 and 2.59 μM) and relative high potency against H1975 (IC<sub>50</sub> = 0.18 and 0.27 μM). Removal of the bromine in **19e** (**19i**) resulted in the significant decrease of selectivity in the kinase assays (68- vs 3-fold), which was similar to our previous observations. The cLogP values of compounds were acceptable according to Lipinski's "Rule of 5" for drug design.

*Please insert Table 3 here*

### 2.5.3. Covalent docking of active compounds **19e** and **19h**

To investigate whether the added acrylamide can form a covalent bond with Cys-797, covalent molecular docking was conducted to predict the binding modes of the representative compounds **19e** and **19h**. The covalent bond was expected to form between the Cys-797 and the added acrylamide group as a spatial constraint in the docking simulation. The results indicated that **19e** and **19h** showed a U-shaped conformation and formed two hydrogen-bonds with the Met793 residue (Figure 4). Similarly, the bromine contacted the mutant Met-790 gatekeeper residue to enhance the potency towards the drug-resistant mutant. The methoxy substituent at R<sup>3</sup> in **19e** and **19h** extended towards Leu-792 and Pro-794 in the hinge region, improving the inhibitory effect. Interestingly, the methyl-indol and dihydro-inden groups at R<sup>2</sup> were

oriented to the hydrophobic pocket of EGFR kinase to contact with the hydrophobic residues, including Leu-718, Phe-723 and Val-726.

To our knowledge, **19e** and **19h** have a unique chemical structure and binding mode compare to other third-generation tyrosine kinase inhibitors reported in the literature. Among these irreversible EGFR mutant kinase inhibitors, only compound **3** incorporated with the electrophilic functionality resides at the same site of **19e** and **19h** on pyrimidine C-2 substituent ring. However, the pyrimidine 4-substituent of **19e** and **19h** is N-linked and with a methyl-indol or dihydro-inden that can extend to the hydrophobic pocket of the kinase domain, whereas the indole group orientation of **3** is adjacent to the gatekeeper residue [21]. Recent studies show that patients treated with **3** exhibit tumor progression and develop drug resistance through mutation of the reactive cysteine to a less nucleophilic serine side chain (EGFR-C797S) [34,35]. Thus, the development of novel molecules with different chemical skeletons like **19e** and **19h** which can efficiently inhibit drug-resistant gatekeeper EGFR mutation will of high clinical value.

*Please insert **Figure 4** here*

#### *2.6. Inhibitory effects of **19e** and **19h** on EGFR activation and downstream signaling transduction in cancer cells*

Potential compounds **19e** and **19h** were selected for validation as well as for evaluating the inhibition of EGFR phosphorylation and downstream signal in H1975

and A431 cells. Our results showed that **19e** and **19h** inhibited the phosphorylation of EGFR<sup>L858R/T790M</sup>, Akt and extracellular signal-regulated kinase (Erk) signaling in a dose-dependent manner (Figure 5). Both compounds inhibited EGFR<sup>L858R/T790M</sup> phosphorylation at 10 nM in EGF-stimulated H1975 cells, similar to compound **3**. However, **19e** and **19h** did not inhibit the phosphorylation of EGFR<sup>WT</sup>, even at 100 nM in A431 cells. The results revealed that **19e** and **19h** were at least 10-fold more potent against EGFR<sup>L858R/T790M</sup> compared to EGFR<sup>WT</sup> in the cell system.

*Please insert **Figure 5** here*

### 2.7. Kinase selectivity profile of **19e** and **19h**

We next investigated the specificity of **19e** and **19h** by profiling their inhibitory activities against a panel of 98 kinases distributed across the whole kinome using the DiscoverX's KINOMEscan platform (Figure 6). The full selectivity profile of compounds can be viewed in the Supporting Information (Table S1). In this panel, the competitive binding of compounds at 1  $\mu$ M was measured as a percentage of control (POC). The results suggested that both compounds displayed excellent selectivity, and the specificity profile of compound **19e** was greater than that of **19h**. **19e** exhibited binding to JAK3 (POC <1%), while compound **19h** also showed strong binding with INSR and JAK2. Other weak off-target binding of **19e** included ALK, ErbB4, INSR, JAK2 and MKNK2 (POC <10%). Compound **19h** also bound to BTK, FAK, IGF1R. In particular, **19e** did not exhibit apparent activity against IGF1R (POC >35%).



Studies have shown that inhibition of IGF1R and INSR signaling lead to hyperglycemia and hyperinsulinemia, which may limit maximal tolerated doses in NSCLC EGFR-sensitive patients [22,36]. Therefore, weak IGF1R and INSR inhibition by **19e** with a 1-methyl-indol group is of great interest. Overall, the high selectivity of **19e** indicated less off-target effects and good safety index for further development.

*Please insert **Figure 6** here*

#### 2.8. *In vivo* pharmacokinetics properties

In view of promising enzymatic and cellular potencies, we performed preliminary pharmacokinetic investigation of the compounds *in vivo* following intravenous (iv) and oral administration. The pharmacokinetic parameters are summarized in Table 4 and Figure S1. Following an oral dose of 10 mg/kg, **19c**, **19e** and **19h** showed a reasonable  $AUC_{0-\infty}$  value of more than 1500 ng·h/mL, moderate  $T_{1/2}$  from 3-5 h, and encouraging oral bioavailability ( $F > 35\%$ ). While **19i**, with no bromine substitution at R<sup>1</sup> position, was found to have low oral bioavailability. These results suggest that these compounds, especially **19c**, **19e** and **19h**, would be suitable for further *in vivo* antitumor studies.

*Please insert **Table 4** here*

### 2.9. *In vivo* antitumor efficacy study

We selected **19e** and **19h** for study of *in vivo* antitumor efficacy using a xenograft mouse model with NCI-H1975 (EGFR<sup>L858R/T790M</sup>) (Figure 7). BALB/c Nude mice (n = 6/group) were administered **19e** and **19h** at 15 and 30 mg/kg (po, once daily) for 18 consecutive days. The tumor weight and growth inhibition (TGI, %) were measured. The results indicated that **19e** and **19h** significantly inhibited tumor growth at either dose as compared to the vehicle group (Figure 7A-D). The TGI values of **19e** were 62% and 86% at 15 and 30 mg/kg/day, respectively; whereas **19h** achieved 61% and 77% at 15 and 30 mg/kg/day, respectively. Significantly, no mortality or significant loss of body weight in any of the treatment groups occurred (Figure S3). Histopathological analyses of vital organs (heart, liver and kidney) also revealed that **19e** and **19h** treatment did not result in toxicity (Figure S2). In addition, **19e** and **19h** significantly decreased the phosphorylated (p)-EGFR level and tumor cell proliferation as shown by reduced Ki-67 staining compared to vehicle groups (Figure 7E-G). The results point to an encouraging *in vivo* antitumor selectivity of **19e** and **19h**. Hence, these compounds are promising candidates for further development as selective EGFR<sup>L858R/T790M</sup> inhibitors.

*Please insert **Figure 7** here*

### 3. Conclusions

We started with a previously reported reversible EGFR inhibitor compound **7**,

and designed and synthesized a series of novel diaminopyrimidine-based EGFR<sup>L858R/T790M</sup> mutant selective inhibitors. The binding mode of **7** with the crystal structure of EGFR<sup>T790M</sup> predicted that introduction of substituents at the 5 position of the pyrimidine scaffold would lead to an increase in both EGFR<sup>L858R/T790M</sup> inhibitory activity and selectivity since this site contacts directly towards the gatekeeper Met790. As expected, introduction of bromine at the 5-position, producing **14g**, resulted in increased EGFR<sup>L858R/T790M</sup> selectivity and inhibitory activity. Modifications of the pyrimidine 4-substituent of **14g** with aromatic heterocycles that extended into the hydrophobic pocket of EGFR kinase further enhanced activity and selectivity. Subsequently, to overcome the high ATP concentration of the cellular milieu, representative compounds (**15a**, **15e**, and **15f**) were then incorporated with the electrophilic functionality residues at the meta-position of the pyrimidine 2-aniline, resulting in promising candidates **19e** and **19h**. Both of these compounds displayed strong anti-growth activities in H1975 cells, and dose-dependently inhibited the phosphorylation of EGFR<sup>L858R/T790M</sup> and downstream signaling pathways. A431 harboring wild-type EGFR was only moderately affected by these compounds. Kinase profiling indicated that **19e** had a good safety index and did not exhibit activities against IGF1R and INSR kinases. Further *in vivo* antitumor evaluation of **19e** and **19h** indicated significant inhibition of tumor growth in the H1975 NSCLC xenograft mouse model using 15 mg/kg/d. In addition, the compounds did not induced toxicity, mortality, or significant body weight loss. With the acceptable pharmacological profile, encouraging selectivity and *in vivo* antitumor effects, compounds **19e** and **19h**

are potential promising candidates for future development of EGFR mutant-sensitive therapies for NSCLC.

#### **4. Experimental section**

#### 4.1. Chemistry

In general, commercial chemicals or solvents were reagent grade and used without further purification. Reagents for synthesis were obtained from Sigma Aldrich and Energy Chemical, whereas Compound **1-3** were purchased from Selleck. All reactions were monitored by thin-layer chromatography (250 silica gel 60 F<sub>254</sub> glass plates). Melting points were determined on a Fisher-Johns melting apparatus and uncorrected. <sup>1</sup>H NMR and <sup>13</sup>C NMR spectra were recorded on a Bruker 600 MHz instrument, and the chemical shifts ( $\delta$ ) were presented as parts per million with TMS as the internal standard. Multiplicities are given as s (singlet), d (doublet), dd (double-doublet), t (triplet), q (quartet), m (multiplet). The spectra data of the target compounds are shown in Supporting Information. Electrospray ionization mass spectra in positive mode (ESI-MS) data were obtained with a Bruker Esquire 3000t spectrometer. Chromatographic purification was carried out on Silica Gel 60 (E.Merck, 70-230 mesh). Analytical HPLC analyses were performed on Agilent 1260 liquid chromatograph fitted with a Inertex-C18 column, with the purity of compounds >95%.

##### 4.1.1. General procedure for preparation of intermediates **10a-10i**, **11a-11j**

Five mmol 2,4-dichloro-5-substitued-pyrimidines (**8a-8g**) or 4,6-dichloro-1*H*-pyrazolo[3,4-*d*]pyrimidine (**8h**) and DIPEA (1.2 mL, 7.5 mmol) were dissolved in DMF (4 mL) and cooled to -60 °C. Indol-5-amine or amines **9a-9i** (5 mmol) dissolved in DMF (2 mL) were added dropwise. The reaction mixture was stirred at -60 °C for about 1 h. Next, the cooling bath was removed, the reaction

mixture was stirred at room temperature for 2 h, and was poured to 10 mL cooled water after the reaction was complete as monitored by TLC. The formed precipitate was collected by filtration, washed with ethanol yielding compounds **10a-10h**, **11a-11j**, which were dried and used in the next step without further purification.

#### 4.1.2. 4-(4-Methylpiperazin-1-yl)phenylamine (**13**) [30]

A solution of 4-fluoronitrobenzene (7.05 g, 50 mmol), and K<sub>2</sub>CO<sub>3</sub> (6.91 g, 50 mmol) in DMSO (10 mL) was stirred at room temperature for 0.5 h. Subsequently, 1-methylpiperazine (8.3 mL, 75 mmol) was added dropwise, and stirred overnight. The mixture was then poured into ice-water, and the yellow precipitate collected by filtration to give **12** and dried. Compound **12** (2.2 g, 10 mmol) was dissolved in methanol (60 mL), 10% Pd/C (0.3 g) added, and stirred at room temperature under an atmosphere of H<sub>2</sub> overnight. After completion of the reaction, the resulting mixture was filtered, and concentrated under vacuum to yield compound **13** as a purple solid. ESI-MS *m/z*: 192.3 (M + H)<sup>+</sup>, calcd for C<sub>11</sub>H<sub>17</sub>N<sub>3</sub>: 191.14.

#### 4.1.3. General procedure for synthesis of Compounds **14a-14h**, **15a-15j**

*N*<sup>4</sup>-(1H-indol-5-yl)-*N*<sup>2</sup>-(4-(4-methylpiperazin-1-yl)phenyl)pyrimidine-2,4-diamine

(**14a**). Compound **10a** (171 mg, 0.7 mmol) and **13** (95 mg, 0.5 mmol) were dissolved in 2-butanol (200 mL). TFA (0.06 mL) was added and stirred at 100 °C for 3 h. Afterwards, the resulting mixture was extracted with EtOAc (3 × 25 mL), washed with brine, dried over anhydrous Na<sub>2</sub>SO<sub>4</sub> and concentrated. The resulting residue was purified by flash chromatography to give **14a** (White powder, 87.5 mg, 44.5 % yield). m.p: 195.6-196.9 °C. <sup>1</sup>H NMR (600 MHz, DMSO-*d*<sub>6</sub>)  $\delta$  (ppm): 10.968 (s, 1H,

indol-H1), 8.982 (s, 1H, -NH-), 8.749 (s, 1H, -NH-), 8.875 (s, 1H, Ar-H), 7.859 (d,  $J = 5.4$  Hz, 1H, H-6), 7.555 (d,  $J = 9.0$  Hz, 2H, Ar-H), 7.294-7.319 (m, 2H, Ar-H, indol-H2), 7.145 (d,  $J = 7.2$  Hz, 1H, Ar-H), 6.798 (d,  $J = 9.0$  Hz, 2H, Ar-H), 6.340 (d,  $J = 2.4$  Hz, 1H, indol-H3), 6.052 (d,  $J = 5.4$  Hz, 1H, H-5), 3.045 (t,  $J = 4.2$  Hz, 4H, piperazine-H $\times$ 4), 2.526 (t,  $J = 4.2$  Hz, 4H, piperazine-H $\times$ 4), 2.267 (s, 3H, N-CH<sub>3</sub>). <sup>13</sup>C NMR (150 MHz, DMSO-*d*<sub>6</sub>)  $\delta$  161.35, 160.13, 155.71, 145.74, 133.69, 132.78, 131.81, 129.564, 127.96, 125.92, 120.66 $\times$ 2, 116.82, 116.14 $\times$ 2, 112.747, 111.41, 101.18, 54.73 $\times$ 2, 49.03 $\times$ 2, 45.63. ESI-MS  $m/z$ : 400.2 (M + H)<sup>+</sup>, calcd for C<sub>23</sub>H<sub>25</sub>N<sub>7</sub>: 399.21.

#### 4.1.3.1.

*N*<sup>4</sup>-(1*H*-indol-5-yl)-*N*<sup>2</sup>-(4-(4-methylpiperazin-1-yl)phenyl)-5-(trifluoromethyl)pyrimidine-2,4-diamine (**14b**). <sup>1</sup>H NMR (500 MHz, DMSO-*d*<sub>6</sub>)  $\delta$  (ppm): 11.147 (s, 1H, indol-H1), 9.339 (s, 1H, -NH-), 8.633 (s, 1H, -NH-), 8.242 (s, 1H, H-6), 7.563 (s, 1H, Ar-H), 7.412 (d,  $J = 8.5$  Hz, 1H, Ar-H), 7.386 (t,  $J = 2.5$  Hz, 1H, indol-H2), 7.244 (d,  $J = 8.5$  Hz, 2H, Ar-H), 7.061 (d,  $J = 7.5$  Hz, 1H, Ar-H), 6.442 (d,  $J = 2.0$  Hz, 1H, indol-H3), 6.374 (d,  $J = 8.5$  Hz, 2H, Ar-H), 2.921 (t,  $J = 4.0$  Hz, 4H, piperazine-H $\times$ 4), 2.426 (t,  $J = 4.0$  Hz, 4H, piperazine-H $\times$ 4), 2.219 (s, 3H, N-CH<sub>3</sub>). <sup>13</sup>C NMR (125 MHz, DMSO-*d*<sub>6</sub>)  $\delta$  160.52, 155.05, 146.02, 134.08, 131.87, 129.74, 128.35, 127.65, 126.20, 125.70 $\times$ 2, 120.66, 120.42, 115.32 $\times$ 2, 111.01, 109.28, 107.74, 101.30, 98.42, 54.58 $\times$ 2, 48.67 $\times$ 2, 45.69. ESI-MS  $m/z$ : 448.5 (M + H)<sup>+</sup>, calcd for C<sub>24</sub>H<sub>24</sub>F<sub>3</sub>N<sub>7</sub>: 467.20.

#### 4.1.3.2.

*N*<sup>4</sup>-(1*H*-indol-5-yl)-*N*<sup>2</sup>-(4-(4-methylpiperazin-1-yl)phenyl)-5-nitropyrimidine-2,4-diam

*ine (14c)*. Red powder, 53.5% yield. m.p: 233.4-235.2 °C. <sup>1</sup>H NMR (600 MHz, DMSO-*d*<sub>6</sub>) δ (ppm): 11.205 (s, 1H, indol-H1), 10.372 (s, 1H, -NH-), 10.209 (s, 1H, -NH-), 9.039 (s, 1H, H-6), 7.776 (s, 1H, Ar-H), 7.436 (d, *J*=8.4 Hz, 1H, Ar-H), 7.417 (t, *J*=2.4 Hz, 1H, indol-H2), 7.345 (d, *J*=9.0 Hz, 2H, Ar-H), 7.152 (d, *J*=8.4 Hz, 1H, Ar-H), 6.509 (d, *J*=9.0 Hz, 2H, Ar-H), 6.442 (d, *J*=2.4 Hz, 1H, indol-H3), 2.993 (t, *J*=4.8 Hz, 4H, piperazine-H×4), 2.457 (t, *J*=4.8 Hz, 4H, piperazine-H×4), 2.241 (s, 3H, N-CH<sub>3</sub>). <sup>13</sup>C NMR (150 MHz, DMSO-*d*<sub>6</sub>) δ 159.58, 158.08, 155.57, 147.71, 134.80, 130.94, 129.27, 128.27, 126.74, 122.08×2, 120.52, 119.86, 117.40, 115.70×2, 111.95, 102.01, 55.10×2, 48.84×2, 46.27. ESI-MS *m/z*: 445.3 (M + H)<sup>+</sup>, calcd for C<sub>23</sub>H<sub>24</sub>N<sub>8</sub>O<sub>2</sub>: 444.20.

#### 4.1.3.3.

*N*<sup>4</sup>-(1*H*-indol-5-yl)-5-methoxy-*N*<sup>2</sup>-(4-(4-methylpiperazin-1-yl)phenyl)pyrimidine-2,4-*d*iamine (**14d**). White powder, 42.0% yield. m.p: 233.4-235.2 °C. <sup>1</sup>H NMR (600 MHz, DMSO-*d*<sub>6</sub>) δ (ppm): 10.975 (s, 1H, indol-H1), 8.516 (s, 1H, -NH-), 8.405 (s, 1H, -NH-), 8.005 (s, 1H, Ar-H), 7.723 (s, 1H, H-6), 7.517 (d, *J*=9.0 Hz, 2H, Ar-H), 7.311-7.355 (m, 3H, indol-H2, Ar-H), 6.727 (d, *J*=9.0 Hz, 2H, Ar-H), 6.349 (d, *J*=2.4 Hz, 1H, indol-H3), 3.824 (s, 3H, -OCH<sub>3</sub>), 2.985 (t, *J*=4.8 Hz, 4H, piperazine-H×4), 2.439 (t, *J*=4.8 Hz, 4H, piperazine-H×4), 2.207 (s, 3H, N-CH<sub>3</sub>). <sup>13</sup>C NMR (150 MHz, DMSO-*d*<sub>6</sub>) δ 154.51, 152.50, 145.32, 136.21, 134.40, 132.92, 131.34, 127.75, 125.78, 124.765, 119.62×2, 117.54, 116.20×2, 113.39, 111.04, 101.24, 57.06, 54.96×2, 49.39×2, 45.95. ESI-MS *m/z*: 430.3 (M + H)<sup>+</sup>, calcd for C<sub>24</sub>H<sub>27</sub>N<sub>7</sub>O: 429.22.



## 4.1.3.4.

*N*<sup>4</sup>-(1*H*-indol-5-yl)-5-methyl-*N*<sup>2</sup>-(4-(4-methylpiperazin-1-yl)phenyl)pyrimidine-2,4-diamine (**14e**). White powder, 35.0% yield. m.p: 262.65-263.8 °C. <sup>1</sup>H NMR (600 MHz, DMSO-*d*<sub>6</sub>) δ (ppm): 11.003 (s, 1H, indol-H1), 8.553(s, 1H, -NH-), 8.099 (s, 1H, -NH-), 7.820 (s, 1H, H-6), 7.759 (s, 1H, Ar-H), 7.472 (d, *J* = 9.0 Hz, 2H, Ar-H), 7.351 (d, *J* = 8.4 Hz, 1H, Ar-H), 7.328 (t, *J* = 2.4 Hz, 1H, indol-H2), 7.250 (d, *J* = 9.0 Hz, 1H, Ar-H), 6.651 (d, *J* = 8.4 Hz, 2H, Ar-H), 6.387 (d, *J* = 2.4 Hz, 1H, indol-H3), 2.971 (t, *J* = 4.2 Hz, 4H, piperazine-H×4), 2.449 (t, *J* = 4.2 Hz, 4H, piperazine-H×4), 2.223 (s, 3H, -NCH<sub>3</sub>), 2.089 (s, 3H, -CH<sub>3</sub>). <sup>13</sup>C NMR (150 MHz, DMSO-*d*<sub>6</sub>) δ 159.93, 158.53, 154.88, 145.10, 133.87, 132.98, 131.38, 127.52, 125.47, 119.58×2, 118.65, 115.87×2, 114.79, 110.71, 104.26, 101.04, 54.70×2, 49.11×2, 45.71, 13.57. ESI-MS *m/z*: 414.1 (M + H)<sup>+</sup>, calcd for C<sub>24</sub>H<sub>27</sub>N<sub>7</sub>: 413.23.

## 4.1.3.5.

5-fluoro-*N*<sup>4</sup>-(1*H*-indol-5-yl)-*N*<sup>2</sup>-(4-(4-methylpiperazin-1-yl)phenyl)pyrimidine-2,4-diamine (**14f**). White powder, 40.5% yield. m.p: 216.8-218.1 °C. <sup>1</sup>H NMR (600 MHz, DMSO-*d*<sub>6</sub>) δ (ppm): 11.022 (s, 1H, indol-H1), 9.071 (s, 1H, -NH-), 8.804 (s, 1H, -NH-), 7.966 (d, *J* = 3.0 Hz, 1H, indol-H3), 7.942 (s, 1H, H-6), 7.480 (d, *J* = 8.4 Hz, 2H, Ar-H), 7.309-7.335 (m, 3H, indol-H2, Ar-H), 6.744 (d, *J* = 8.4 Hz, 2H, Ar-H), 6.382 (s, 1H, Ar-H), 3.020 (t, *J* = 4.2 Hz, 4H, piperazine-H×4), 2.510 (t, *J* = 4.2 Hz, 4H, piperazine-H×4), 2.249 (s, 3H, N-CH<sub>3</sub>). <sup>13</sup>C NMR (150 MHz, DMSO-*d*<sub>6</sub>) δ 171.98, 155.94, 150.22, 145.53, 141.14, 139.64, 133.18 (d, *J*<sub>C-F</sub> = 277.8 Hz), 130.47, 127.51, 125.70, 120.00×2, 117.43, 115.84×2, 113.66, 110.91, 101.06, 54.60×2,

48.90×2, 45.57. ESI-MS  $m/z$ : 418.1 (M + H)<sup>+</sup>, calcd for C<sub>23</sub>H<sub>24</sub>FN<sub>7</sub>: 417.20.

#### 4.1.3.6.

*5-bromo-N<sup>4</sup>-(1H-indol-5-yl)-N<sup>2</sup>-(4-(4-methylpiperazin-1-yl)phenyl)pyrimidine-2,4-diamine (14g)*. White powder, 35.2% yield. m.p: 204.6-206.2 °C. <sup>1</sup>H NMR (600 MHz, DMSO-*d*<sub>6</sub>)  $\delta$  (ppm): 11.079 (s, 1H, indol-H1), 8.924 (s, 1H, -NH-), 8.393 (s, 1H, -NH-), 8.063 (s, 1H, H-6), 7.683 (s, 1H, Ar-H), 7.340-7.368 (m, 4H, Ar-H, indol-H2), 7.147 (d,  $J$  = 8.4 Hz, 1H, Ar-H), 6.572 (d,  $J$  = 7.2 Hz, 2H, Ar-H), 6.391 (d,  $J$  = 2.4 Hz, 1H, indol-H3), 2.985 (t,  $J$  = 4.2 Hz, 4H, piperazine-H×4), 2.545 (t,  $J$  = 4.2 Hz, 4H, piperazine-H×4), 2.290 (s, 3H, -NCH<sub>3</sub>). <sup>13</sup>C NMR (150 MHz, DMSO-*d*<sub>6</sub>)  $\delta$  157.92, 156.60, 153.89, 144.66, 133.51, 130.07, 127.50, 125.74, 123.25, 120.16×2, 119.06, 116.15×2, 115.79, 110.90, 102.85, 101.16, 52.99×2, 47.19×2, 44.12. ESI-MS  $m/z$ : 478.1 (M + H)<sup>+</sup>, calcd for C<sub>23</sub>H<sub>24</sub>BrN<sub>7</sub>: 477.12.

#### 4.1.3.7.

*N<sup>4</sup>-(1H-indol-5-yl)-N<sup>6</sup>-(4-(4-methylpiperazin-1-yl)phenyl)-1H-pyrazolo[3,4-*d*]pyrimidine-4,6-diamine(14h)*. Compound

6-chloro-*N*-(1H-indol-5-yl)-1H-pyrazolo[3,4-*d*]pyrimidin-4-amine (**10h**, 199 mg, 0.7 mmol) and **13** (95 mg, 0.5 mmol) were dissolved in 2-pentanol (50 mL). Toluenesulfonic acid monohydrate (95mg, 0.5 mmol) was added and stirred at 120 °C for 5 h. The resulting mixture was extracted with EtOAc (3 × 25 mL), washed with brine, dried over anhydrous Na<sub>2</sub>SO<sub>4</sub> and concentrated. The resulting residue was purified by flash chromatography to give **14h** (Red powder, 125 mg, 57.3 % yield). m.p: 247.5-249.0 °C <sup>1</sup>H NMR (600 MHz, DMSO-*d*<sub>6</sub>)  $\delta$  (ppm): 12.758 (s, 1H,

pyrazolo-H1), 11.079 (s, 1H, indol-H1), 9.484 (s, 1H, -NH-), 8.786 (s, 1H, -NH-), 8.031 (s, 1H, pyrazolo-H3), 7.629 (d,  $J = 7.2$  Hz, 2H, Ar-H), 7.351-7.397 (m, 3H, Ar-H, indol-H2), 7.352 (s, 1H, Ar-H), 6.83 (d,  $J = 8.4$  Hz, 2H, Ar-H), 6.415 (d,  $J = 2.4$  Hz, 1H, indol-H3), 3.135 (s, 4H, piperazine-H $\times$ 4), 2.730 (s, 4H, piperazine-H $\times$ 4), 2.412 (s, 3H, -NCH<sub>3</sub>). <sup>13</sup>C NMR (150 MHz, DMSO-*d*<sub>6</sub>)  $\delta$  158.79, 156.95, 145.18, 142.10, 139.79, 133.79, 133.21, 133.08, 132.68, 131.09, 129.45, 127.68, 125.82, 120.58 $\times$ 2, 116.02 $\times$ 2, 111.15, 101.20, 53.95 $\times$ 2, 48.20 $\times$ 2, 45.47. ESI-MS  $m/z$ : 440.2 (M+H)<sup>+</sup>, calcd for C<sub>24</sub>H<sub>25</sub>N<sub>9</sub>: 439.22.

#### 4.1.3.8.

*5-Bromo-N<sup>4</sup>-(1H-indol-6-yl)-N<sup>2</sup>-(4-(4-methylpiperazin-1-yl)phenyl)pyrimidine-2,4-diamine (15a)*. White powder, 40.5% yield, m.p: 178.7-180.2 °C. <sup>1</sup>H NMR (600 MHz, DMSO-*d*<sub>6</sub>)  $\delta$  (ppm): 11.082 (s, 1H, indole-H-1), 8.964 (s, 1H, -NH-), 8.512 (s, 1H, -NH-), 8.104 (s, 1H, H-6), 7.517 (d,  $J = 8.4$  Hz, 2H, Ar-H), 7.374 (d,  $J = 8.4$  Hz, 2H, Ar-H), 7.332 (t,  $J = 3.0$  Hz, 1H, indole-H-2), 7.125 (d,  $J = 8.4$  Hz, 1H, Ar-H), 6.575 (d,  $J = 5.4$  Hz, 2H, Ar-H), 6.437-6.443 (m, 1H, indole-H-3), 2.954 (t,  $J = 4.2$  Hz, 4H, piperazine-H $\times$ 4), 2.450 (t,  $J = 4.2$  Hz, 4H, piperazine-H $\times$ 4), 2.225 (s, 3H, N-CH<sub>3</sub>). <sup>13</sup>C NMR (150 MHz, DMSO-*d*<sub>6</sub>)  $\delta$  158.30, 157.39, 156.95, 145.64, 135.85, 132.76, 132.28, 125.34, 125.15, 120.06 $\times$ 2, 119.41, 117.28, 115.67 $\times$ 2, 108.07, 100.95, 91.82, 54.57 $\times$ 2, 48.79 $\times$ 2, 45.61. ESI-MS  $m/z$ : 478.1 (M + H)<sup>+</sup>, calcd for C<sub>23</sub>H<sub>24</sub>BrN<sub>7</sub>: 477.12.

#### 4.1.3.9.

*5-Bromo-N<sup>4</sup>-(1H-indazol-5-yl)-N<sup>2</sup>-(4-(4-methylpiperazin-1-yl)phenyl)pyrimidine-2,4-*

*diamine(15b)*. White powder, 36.8 % yield, m.p: 219.4-219.7 °C. <sup>1</sup>H NMR (600 MHz, DMSO-*d*<sub>6</sub>) δ (ppm): 13.049 (s, 1H, indazol-H-1), 8.987 (s, 1H, -NH-), 8.568 (s, 1H, -NH-), 8.116 (s, 1H, H-6), 8.014 (s, 1H, indazol-H-3), 7.941 (s, 1H, Ar-H), 7.523 (d, *J* = 8.4 Hz, 1H, Ar-H), 7.452 (d, *J* = 8.4 Hz, 1H, Ar-H) , 7.325 (d, *J* = 7.8 Hz, 2H, Ar-H), 6.599 (d, *J* = 5.4 Hz, 2H, Ar-H), 2.965 (t, *J* = 4.2 Hz, 4H, piperazine-H×4), 2.425 (t, *J* = 4.2 Hz, 4H, piperazine-H×4), 2.208 (s, 3H, N-CH<sub>3</sub>). <sup>13</sup>C NMR (150 MHz, DMSO-*d*<sub>6</sub>) δ 158.37, 157.22, 157.09, 145.95, 137.59, 133.40, 132.50, 131.50, 124.71, 122.80, 120.52×2, 115.56×2, 115.20, 109.70, 91.67, 54.67×2, 48.84×2, 45.76. ESI-MS *m/z*: 479.2 (M + H)<sup>+</sup>, calcd for C<sub>22</sub>H<sub>23</sub>BrN<sub>8</sub>: 478.12.

#### 4.1.3.10.

*5-bromo-N<sup>4</sup>-(1H-indazol-6-yl)-N<sup>2</sup>-(4-(4-methylpiperazin-1-yl)phenyl)pyrimidine-2,4-diamine(15c)*. White powder, 63.5% yield, m.p: 221.2-223.5 °C. <sup>1</sup>H NMR (600 MHz, DMSO-*d*<sub>6</sub>) δ (ppm): 12.951 (s, 1H, indazol-H-1), 9.063 (s, 1H, -NH-), 8.645 (s, 1H, -NH-), 8.163 (s, 1H, H-6), 8.033 (s, 1H, indazol-H-3), 7.706 (d, *J* = 8.4 Hz, 1H, Ar-H), 7.695 (s, 1H, Ar-H), 7.384 (d, *J* = 9.0 Hz, 2H, Ar-H) , 7.313 (d, *J* = 8.4 Hz, 1H, Ar-H), 6.645 (d, *J* = 7.8 Hz, 2H, Ar-H), 2.971 (t, *J* = 4.2 Hz, 4H, piperazine-H×4), 2.428 (t, *J* = 4.2 Hz, 4H, piperazine-H×4), 2.210 (s, 3H, N-CH<sub>3</sub>). <sup>13</sup>C NMR (150 MHz, DMSO-*d*<sub>6</sub>) δ 158.28, 157.46, 156.95, 145.96, 140.15, 136.84, 133.30, 132.45, 120.29×2, 119.92, 118.42, 117.82, 115.65×2, 104.33, 92.03, 54.64×2, 48.81×2, 45.73. ESI-MS *m/z*: 479.1 (M + H)<sup>+</sup>, calcd for C<sub>22</sub>H<sub>23</sub>BrN<sub>8</sub>: 478.12.

#### 4.1.3.11.

*5-bromo-N<sup>4</sup>-(1-(3-fluorobenzyl)-1H-indol-5-yl)-N<sup>2</sup>-(4-(4-methylpiperazin-1-yl)phenyl)*

*pyrimidine-2,4-diamine (15d)*. Yellow powder, 60.9 % yield, m.p: 188.7-189.3 °C. <sup>1</sup>H NMR (600 MHz, DMSO-*d*<sub>6</sub>) δ (ppm): 8.959 (s, 1H, -NH-), 8.420 (s, 1H, -NH-), 8.091 (s, 1H, H-6), 7.767 (s, 1H, Ar-H), 7.539 (d, *J* = 3.0 Hz, 1H, indole-H-2), 7.438 (d, *J* = 9.0 Hz, 1H, Ar-H), 7.320-7.383 (m, 3H, Ar-H), 7.223 (t, *J* = 9.0 Hz, 1H, Ar-H), 6.992-7.090 (m, 3H, Ar-H), 6.599 (d, *J* = 6.6 Hz, 2H, Ar-H), 6.495 (d, *J* = 3.0 Hz, 1H, indole-H-3), 5.469 (s, 2H, -CH<sub>2</sub>-Ph), 2.941 (t, *J* = 4.2 Hz, 4H, piperazine-H×4), 2.422 (t, *J* = 4.2 Hz, 4H, piperazine-H×4), 2.212 (s, 3H, N-CH<sub>3</sub>). <sup>13</sup>C NMR (150 MHz, DMSO-*d*<sub>6</sub>) δ 163.03, 161.41, 157.76 (d, *J*<sub>C-F</sub>=198.0 Hz), 156.84, 145.76, 141.35 (d, *J*<sub>C-F</sub>=22.8 Hz), 133.41, 132.63, 130.71, 130.49 (d, *J*<sub>C-F</sub>=31.8 Hz), 129.55, 128.17, 122.84, 120.29×2, 119.36, 116.39, 115.62×2, 114.09 (d, *J*<sub>C-F</sub>=84.0 Hz), 113.60 (d, *J*<sub>C-F</sub>=90.0 Hz), 109.61, 101.40, 91.73, 54.61×2, 48.79×2, 48.56, 45.68. ESI-MS *m/z*: 586.2 (M + H)<sup>+</sup>, calcd for C<sub>30</sub>H<sub>29</sub>BrFN<sub>7</sub>: 585.16.

#### 4.1.3.12.

*5-bromo-N<sup>4</sup>-(1-methyl-1H-indol-6-yl)-N<sup>2</sup>-(4-(4-methylpiperazin-1-yl)phenyl)pyrimidine-2,4-diamine (15e)*. White powder, 53.4 % yield, m.p: 176.5-177.2 °C. <sup>1</sup>H NMR (600 MHz, DMSO-*d*<sub>6</sub>) δ (ppm): 8.999 (s, 1H, -NH-), 8.508 (s, 1H, -NH-), 8.120 (s, 1H, H-6), 7.642 (s, 1H, Ar-H), 7.510 (d, *J* = 8.4 Hz, 1H, Ar-H), 7.361 (d, *J* = 8.4 Hz, 2H, Ar-H), 7.304 (d, *J* = 3.0 Hz, 1H, indole-H-2), 7.171 (d, *J* = 8.4 Hz, 1H, Ar-H), 6.555 (d, *J* = 6.0 Hz, 2H), 6.422 (d, *J* = 2.4 Hz, 1H, indole-H-3), 3.676 (s, 3H, indole-N-CH<sub>3</sub>), 2.954 (t, *J* = 4.2 Hz, 4H, piperazine-H×4), 2.436 (t, *J* = 4.2 Hz, 4H, piperazine-H×4), 2.217 (s, 3H, N-CH<sub>3</sub>). <sup>13</sup>C NMR (150 MHz, DMSO-*d*<sub>6</sub>) δ 158.27, 157.12, 156.99, 145.77, 136.34, 132.63, 129.59, 125.23, 125.20, 120.22×2, 119.78,

116.83, 115.52×2, 105.65, 100.25, 91.79, 54.62×2, 48.82×2, 45.69, 32.46. ESI-MS  $m/z$ : 492.2 (M + H)<sup>+</sup>, calcd for C<sub>24</sub>H<sub>26</sub>BrN<sub>7</sub>: 491.14.

#### 4.1.3.13.

*5-bromo-N<sup>4</sup>-(2,3-dihydro-1H-inden-5-yl)-N<sup>2</sup>-(4-(4-methylpiperazin-1-yl)phenyl)pyrimidine-2,4-diamine (15f)*. White powder, 50.9 % yield, m.p: 179.2-180.4 °C. <sup>1</sup>H NMR (600 MHz, DMSO-*d*<sub>6</sub>) δ (ppm): 9.042 (s, 1H, -NH-), 8.342 (s, 1H, -NH-), 8.116 (s, 1H, H-6), 7.494 (s, 1H, Ar-H), 7.394 (d, *J* = 9.0 Hz, 2H, Ar-H), 7.278 (d, *J* = 7.2 Hz, 1H, Ar-H), 7.175 (d, *J* = 8.4 Hz, 1H, Ar-H), 6.735 (d, *J* = 9.0 Hz, 2H, Ar-H), 3.016 (t, *J* = 4.8 Hz, 4H, piperazine-H×4), 2.850 (t, *J* = 7.8 Hz, 2H, dihydro-inden-CH<sub>2</sub>), 2.835 (t, *J* = 7.8 Hz, 2H, dihydro-inden-CH<sub>2</sub>), 2.432 (t, *J* = 4.8 Hz, 4H, piperazine-H×4), 2.205 (s, 3H, N-CH<sub>3</sub>), 2.013-2.062 (m, 2H, dihydro-inden-CH<sub>2</sub>). <sup>13</sup>C NMR (150 MHz, DMSO-*d*<sub>6</sub>) δ 158.37, 157.19, 156.64, 146.05, 143.75, 139.20, 136.81, 132.44, 123.79, 121.43, 120.65×2, 119.62, 115.63×2, 91.83, 54.69×2, 48.87×2, 45.76, 32.56, 31.88, 25.33. ESI-MS  $m/z$ : 480.5 (M + H)<sup>+</sup>, calcd for C<sub>24</sub>H<sub>27</sub>BrN<sub>6</sub>: 479.42.

#### 4.1.3.14.

*1-(5-((5-bromo-2-((4-(4-methylpiperazin-1-yl)phenyl)amino)pyrimidin-4-yl)amino)indolin-1-yl)ethan-1-one (15g)*. White powder, 25.7 % yield, m.p: 220.5-221.7 °C. <sup>1</sup>H NMR (600 MHz, DMSO-*d*<sub>6</sub>) δ (ppm): 9.026 (s, 1H, -NH-), 8.401 (s, 1H, -NH-), 8.110 (s, 1H, H-6), 7.991 (d, *J* = 9.0 Hz, 1H, Ar-H), 7.513 (s, 1H, Ar-H), 7.380 (d, *J* = 8.4 Hz, 2H, Ar-H), 7.324 (d, *J* = 7.2 Hz, 1H, Ar-H), 6.751 (d, *J* = 9.0 Hz, 2H, Ar-H), 4.110 (t, *J* = 8.4 Hz, 2H, indolin-CH<sub>2</sub>), 3.108 (t, *J* = 8.4 Hz, 2H, indolin-CH<sub>2</sub>), 3.030 (t, *J* = 4.2 Hz, 4H, piperazine-H×4), 2.462 (t, *J* = 4.2 Hz, 4H, piperazine-H×4), 2.229

(s, 3H, N-CH<sub>3</sub>), 2.160 (s, 3H, -COCH<sub>3</sub>). <sup>13</sup>C NMR (150 MHz, DMSO-*d*<sub>6</sub>) δ 168.08, 158.34, 157.21, 156.56, 146.08, 139.24, 134.04, 132.35, 131.74, 122.12, 120.71×2, 120.17, 115.56×2, 115.38, 91.74, 54.70×2, 48.79×2, 48.32, 45.77, 27.53, 23.83. ESI-MS *m/z*: 522.0 (M + H)<sup>+</sup>, calcd for C<sub>25</sub>H<sub>28</sub>BrN<sub>7</sub>O: 521.15.

#### 4.1.3.15.

*1-(6-((5-bromo-2-((4-(4-methylpiperazin-1-yl)phenyl)amino)pyrimidin-4-yl)amino)indolin-1-yl)ethan-1-one (15h)*. White powder, 38.6 % yield, m.p: 201.3-202.4 °C. <sup>1</sup>H NMR (600 MHz, DMSO-*d*<sub>6</sub>) δ (ppm): 8.984 (s, 1H, -NH-), 8.544 (s, 1H, -NH-), 8.112 (s, 1H, H-6), 8.098 (s, 1H, Ar-H), 7.380 (d, *J* = 8.4 Hz, 2H, Ar-H), 7.182-7.224 (m, 2H, Ar-H), 6.683 (d, *J* = 8.4 Hz, 2H, Ar-H), 4.139 (t, *J* = 9.0 Hz, 2H, indolin-CH<sub>2</sub>), 3.149 (t, *J* = 8.4 Hz, 2H, indolin-CH<sub>2</sub>), 3.004 (t, *J* = 4.8 Hz, 4H, piperazine-H×4), 2.438 (t, *J* = 4.8 Hz, 4H, piperazine-H×4), 2.210 (s, 3H, N-CH<sub>3</sub>), 2.157 (s, 3H, -COCH<sub>3</sub>). <sup>13</sup>C NMR (150 MHz, DMSO-*d*<sub>6</sub>) δ 168.31, 158.25, 157.28, 157.06, 145.94, 142.94, 137.45, 132.47, 127.70, 124.04, 120.39×2, 119.37, 115.55×2, 112.56, 91.82, 54.68×2, 48.91×2, 48.80, 45.73, 27.09, 23.97. ESI-MS *m/z*: 522.1 (M + H)<sup>+</sup>, calcd for C<sub>25</sub>H<sub>28</sub>BrN<sub>7</sub>O: 521.15.

#### 4.1.3.16.

*5-bromo-N<sup>2</sup>-(4-(4-methylpiperazin-1-yl)phenyl)-N<sup>4</sup>-(quinolin-6-yl)pyrimidine-2,4-diamine (15i)*. Yellow powder, 57.3 % yield, m.p: 214.2-214.7 °C. <sup>1</sup>H NMR (600 MHz, DMSO-*d*<sub>6</sub>) δ (ppm): 9.148 (s, 1H -NH-), 8.807 (d, *J* = 3.0 Hz, 1H, quinolin-H-2), 8.767 (s, 1H -NH-), 8.370 (s, 1H, Ar-H), 8.219 (s, 1H, H-6), 8.151 (s, 1H, Ar-H), 7.919-7.994 (m, 2H, quinolin-H-4, Ar-H), 7.463-7.484 (m, 1H, quinolin-H-3), 7.384

(d,  $J = 7.2$  Hz, 2H, Ar-H), 6.710 (d,  $J = 6.6$  Hz, 2H, Ar-H), 3.004 (t,  $J = 4.8$  Hz, 4H, piperazine-H $\times$ 4), 2.444 (t,  $J = 4.8$  Hz, 4H, piperazine-H $\times$ 4), 2.219 (s, 3H, N-CH<sub>3</sub>).  
<sup>13</sup>C NMR (150 MHz, DMSO-*d*<sub>6</sub>)  $\delta$  158.53, 157.81, 156.42, 149.10, 146.39, 144.90, 136.93, 135.47, 132.03, 128.78, 128.02, 126.55, 121.43, 121.36 $\times$ 2, 118.66, 115.62 $\times$ 2, 92.05, 54.66 $\times$ 2, 48.72 $\times$ 2, 45.75. ESI-MS  $m/z$ : 490.1 (M + H)<sup>+</sup>, calcd for C<sub>24</sub>H<sub>24</sub>BrN<sub>7</sub>: 489.12.

#### 4.1.3.17.

*5-bromo-N<sup>2</sup>-(4-(4-methylpiperazin-1-yl)phenyl)-N<sup>4</sup>-(quinoxalin-6-yl)pyrimidine-2,4-diamine (15j)*. Yellow powder, 42.1 % yield, m.p: 193.6-195.3 °C. <sup>1</sup>H NMR (600 MHz, DMSO-*d*<sub>6</sub>)  $\delta$  (ppm): 9.233 (s, 1H, -NH-), 8.959 (s, 1H, -NH-), 8.889 (d,  $J = 1.8$  Hz, 1H, quinoxalin-H), 8.836 (d,  $J = 1.8$  Hz, 1H, quinoxalin-H), 8.445 (s, 1H, Ar-H), 8.265 (s, 1H, H-6), 8.206 (d,  $J = 8.4$  Hz, 1H, Ar-H), 8.016 (d,  $J = 9.0$  Hz, 1H, Ar-H), 7.430 (d,  $J = 8.4$  Hz, 2H, Ar-H), 6.755 (d,  $J = 8.4$  Hz, 2H, Ar-H), 3.013 (t,  $J = 4.2$  Hz, 4H, piperazine-H $\times$ 4), 2.452 (t,  $J = 4.2$  Hz, 4H, piperazine-H $\times$ 4), 2.224 (s, 3H, N-CH<sub>3</sub>).  
<sup>13</sup>C NMR (150 MHz, DMSO-*d*<sub>6</sub>)  $\delta$  158.39, 158.16, 156.26, 146.29, 145.64, 143.96, 142.85, 140.44, 139.30, 132.01, 128.65, 126.94, 118.76, 120.99 $\times$ 2, 115.76 $\times$ 2, 92.43, 54.62 $\times$ 2, 48.74 $\times$ 2, 45.70. ESI-MS  $m/z$ : 491.1 (M + H)<sup>+</sup>, calcd for C<sub>23</sub>H<sub>23</sub>BrN<sub>8</sub>: 490.12.

#### 4.1.4. General procedure for the preparation of the intermediates **16a-16f**

2-chloropyrimidines (**11a**, **11e**, **11f**) (2 mmol), 4-fluoro-2-substitued-5-nitroaniline (**20a**, **20b**) (2 mmol), and p-toluenesulfonic acid monohydrate (380 mg, 2 mmol) were heated at 120 °C in 2-pentanol (40 mL) for 8 h,



and the resultant mixture was cooled and filtered. The solid was filtered and washed with EtOH, then dried to give yellow crude intermediates **16a-16f**.

#### 4.1.5. General procedure for the preparation of the intermediates **17a-17i**

Crude intermediates **16a-16f** (1 mmol) and amines (1-Methylpiperazine or  $N^1,N^1,N^2$ -trimethylethane-1,2-diamine, 3 mmol) were dissolved in 2-pentanol (50 mL), and the reaction was stirred at 120 °C for 3 h. The reaction mixture was evaporated to dryness, extracted with EtOAc, washed with saturated brine, dried over anhydrous  $\text{Na}_2\text{SO}_4$  and concentrated. The crude product was purified by flash silica chromatography, with an elution gradient of 5% MeOH in EtOAc to give red solid **17a-17i**.

For example:

5-bromo- $N^2$ -(4-((2-(dimethylamino)ethyl)(methyl)amino)-3-nitrophenyl)- $N^4$ -(1*H*-indol-6-yl)pyrimidine-2,4-diamine (**17a**). Red powder, 70.4 % yield  $^1\text{H}$  NMR (600 MHz,  $\text{DMSO}-d_6$ )  $\delta$  (ppm): 11.060 (s, 1H, indole-H-1), 9.361 (s, 1H, -NH-), 8.658 (s, 1H, -NH-), 8.177 (s, 1H, H-6), 7.864 (s, 1H, Ar-H), 7.698 (d,  $J = 9.0$  Hz, 1H, Ar-H), 7.494 (d,  $J = 7.8$  Hz, 1H, Ar-H), 7.453 (s, 1H, Ar-H), 7.325 (t,  $J = 2.4$  Hz, 1H, indole-H-2), 7.105 (d,  $J = 8.4$  Hz, 1H, Ar-H), 6.874 (s, 1H, Ar-H), 6.421-6.429 (m, 1H, indole-H-3), 2.971 (t,  $J = 7.2$  Hz, 2H,  $-\text{CH}_2-\text{CH}_2-\text{N}(\text{CH}_3)_2$ ), 2.634 (s, 3H, N- $\text{CH}_3$ ), 2.971 (t,  $J = 7.2$  Hz, 2H,  $-\text{CH}_2-\text{CH}_2-\text{N}(\text{CH}_3)_2$ ), 2.082 (s, 6H,  $-\text{N}(\text{CH}_3)_2$ ).  $^{13}\text{C}$  NMR (150 MHz,  $\text{DMSO}-d_6$ )  $\delta$  157.89, 157.53, 156.92, 142.61, 138.88, 135.79, 134.38, 131.98, 125.44, 125.31, 123.81, 121.47, 119.44, 117.30, 113.83, 108.07, 100.98, 93.11, 56.55, 53.37, 45.38 $\times$ 2, 41.25. ESI-MS  $m/z$ : 525.0 (M + H) $^+$ , calcd for  $\text{C}_{23}\text{H}_{25}\text{BrN}_8\text{O}_2$ : 524.12.

#### 4.1.6. General procedure for the preparation of the intermediates **18a-18i**

Intermediates **17a-17i** (1.5 mmol), iron (15.0 mmol), and ammonium chloride (1.5 mmol) were mixed in EtOH (30 mL) and water (10 mL) at reflux for 2 h. The mixture was filtered and concentrated. The crude product was purified by flash silica chromatography, eluting with 5% MeOH in ethyl acetate, and the pure fractions were evaporated to yield amines **18a-18i**.

##### 4.1.6.1.

*N<sup>4</sup>-(4-((1H-indol-6-yl)amino)-5-bromopyrimidin-2-yl)-N<sup>1</sup>-(2-(dimethylamino)ethyl)-N<sup>1</sup>-methylbenzene-1,2,4-triamine (18a)*. White powder, 72.5 % yield. <sup>1</sup>H NMR (600 MHz, DMSO-*d*<sub>6</sub>)  $\delta$  (ppm): 11.084 (s, 1H, indole-H-1), 8.848 (s, 1H, -NH-), 8.468 (s, 1H, -NH-), 8.098 (s, 1H, H-6), 7.592 (s, 1H, Ar-H), 7.510 (d, *J* = 8.4 Hz, 1H, Ar-H), 7.315 (t, *J* = 3.0 Hz, 1H, indole-H-2), 7.318 (d, *J* = 8.4 Hz, 1H, Ar-H), 6.877 (s, 1H, Ar-H), 6.673 (d, *J* = 8.4 Hz, 1H, Ar-H), 6.626 (d, *J* = 8.4 Hz, 1H, Ar-H), 6.416 (t, *J* = 2.4 Hz, 1H, indole-H-3), 4.476 (s, 2H, -NH<sub>2</sub>), 2.770 (t, *J* = 7.2 Hz, 2H, -CH<sub>2</sub>-CH<sub>2</sub>-N(CH<sub>3</sub>)<sub>2</sub>), 2.480 (s, 3H, N-CH<sub>3</sub>), 2.254 (t, *J* = 7.2 Hz, 2H, -CH<sub>2</sub>-CH<sub>2</sub>-N(CH<sub>3</sub>)<sub>2</sub>), 2.128 (s, 6H, -N(CH<sub>3</sub>)<sub>2</sub>). <sup>13</sup>C NMR (150 MHz, DMSO-*d*<sub>6</sub>)  $\delta$  158.39, 157.19, 156.88, 142.65, 136.62, 135.76, 133.08, 132.37, 125.34, 124.88, 119.96, 119.36, 117.15, 108.36, 107.72, 105.78, 100.91, 91.82, 57.30, 54.17, 45.66 $\times$ 2, 41.65. ESI-MS *m/z*: 495.0 (M + H)<sup>+</sup>, calcd for C<sub>23</sub>H<sub>27</sub>BrN<sub>8</sub>: 494.15.

##### 4.1.6.2.

*N<sup>2</sup>-(3-amino-4-(4-methylpiperazin-1-yl)phenyl)-5-bromo-N<sup>4</sup>-(1H-indol-6-yl)pyrimidine-2,4-diamine (18b)*. White powder, 67.5 % yield. <sup>1</sup>H NMR (600 MHz, DMSO-*d*<sub>6</sub>)  $\delta$

(ppm): 11.079 (s, 1H, indole-H-1), 8.866 (s, 1H, -NH-), 8.479 (s, 1H, -NH-), 8.097 (s, 1H, H-6), 7.568 (s, 1H, Ar-H), 7.512 (d,  $J = 8.4$  Hz, 1H, Ar-H), 7.325 (t,  $J = 2.4$  Hz, 1H, indole-H-2), 7.132 (d,  $J = 8.4$  Hz, 1H, Ar-H), 6.889 (s, 1H, Ar-H), 6.725 (d,  $J = 8.4$  Hz, 1H, Ar-H), 6.567 (d,  $J = 8.4$  Hz, 1H, Ar-H), 6.429 (t,  $J = 2.4$  Hz, 1H, indole-H-3), 4.240 (s, 2H, -NH<sub>2</sub>), 2.665 (t,  $J = 4.8$  Hz, 4H, piperazine-H $\times$ 4), 2.431 (t,  $J = 4.8$  Hz, 4H, piperazine-H $\times$ 4), 2.208 (s, 3H, N-CH<sub>3</sub>). <sup>13</sup>C NMR (150 MHz, DMSO-*d*<sub>6</sub>)  $\delta$  158.36, 157.21, 156.87, 141.68, 136.72, 135.76, 132.74, 132.33, 125.37, 124.92, 119.37, 118.89, 117.18, 108.57, 107.79, 105.77, 100.96, 91.87, 55.32 $\times$ 2, 50.72 $\times$ 2, 45.86. ESI-MS  $m/z$ : 493.2 (M + H)<sup>+</sup>, calcd for C<sub>23</sub>H<sub>25</sub>BrN<sub>8</sub>: 492.13.

#### 4.1.6.3.

*N*<sup>2</sup>-(5-amino-2-methoxy-4-(4-methylpiperazin-1-yl)phenyl)-5-bromo-*N*<sup>4</sup>-(1H-indol-6-yl)pyrimidine-2,4-diamine (**18c**). White powder, 83.2 % yield. <sup>1</sup>H NMR (500 MHz, DMSO-*d*<sub>6</sub>)  $\delta$  (ppm): 11.143 (s, 1H, indole-H-1), 8.529 (s, 1H, -NH-), 8.115 (s, 1H, H-6), 7.660 (s, 1H, -NH-), 7.510 (d,  $J = 6.0$  Hz, 1H, Ar-H), 7.502 (s, 1H, Ar-H), 7.326 (t,  $J = 2.0$  Hz, 1H, indole-H-2), 7.276 (s, 1H, Ar-H), 7.130 (d,  $J = 7.0$  Hz, 1H, Ar-H), 6.623 (s, 1H, Ar-H), 6.421 (t,  $J = 2.0$  Hz, 1H, indole-H-3), 3.878 (s, 2H, -NH<sub>2</sub>), 3.699 (s, 3H, -OCH<sub>3</sub>), 2.758 (t,  $J = 4.0$  Hz, 4H, piperazine-H $\times$ 4), 2.511 (t,  $J = 4.0$  Hz, 4H, piperazine-H $\times$ 4), 2.266 (s, 3H, N-CH<sub>3</sub>). <sup>13</sup>C NMR (125 MHz, DMSO-*d*<sub>6</sub>)  $\delta$  161.30, 158.26, 157.11, 156.93, 148.86, 143.58, 135.70, 135.08, 134.98, 132.33, 125.39, 124.87, 121.14, 119.39, 116.81, 107.18, 101.01, 93.593, 56.42, 55.16 $\times$ 2, 50.34 $\times$ 2, 45.70. ESI-MS  $m/z$ : 523.1 (M + H)<sup>+</sup>, calcd for C<sub>24</sub>H<sub>27</sub>BrN<sub>8</sub>O: 522.14.

#### 4.1.6.4.

*N*<sup>2</sup>-(3-amino-4-(4-methylpiperazin-1-yl)phenyl)-5-bromo-*N*<sup>4</sup>-(1-methyl-1*H*-indol-6-yl)pyrimidine-2,4-diamine (**18d**). White powder, 80.2 % yield. <sup>1</sup>H NMR (600 MHz, DMSO-*d*<sub>6</sub>) δ (ppm): 8.915 (s, 1H, -NH-), 8.489 (s, 1H, -NH-), 8.118 (s, 1H, H-6), 7.677 (s, 1H, Ar-H), 7.516 (d, *J* = 8.4 Hz, 1H, Ar-H), 7.305 (t, *J* = 3.0 Hz, 1H, indole-H-2), 7.196 (d, *J* = 9.0 Hz, 1H, Ar-H), 6.840 (s, 1H, Ar-H), 6.794 (d, *J* = 9.0 Hz, 1H, Ar-H), 6.518 (d, *J* = 8.4 Hz, 1H, Ar-H), 6.418 (t, *J* = 3.0 Hz, 1H, indole-H-3), 4.279 (s, 2H, -NH<sub>2</sub>), 3.703 (s, 3H, indole-N-CH<sub>3</sub>), 2.672 (t, *J* = 4.2 Hz, 4H, piperazine-H×4), 2.436 (t, *J* = 4.2 Hz, 4H, piperazine-H×4), 2.211 (s, 3H, N-CH<sub>3</sub>). <sup>13</sup>C NMR (150 MHz, DMSO-*d*<sub>6</sub>) δ 157.31, 156.02, 155.89, 140.87, 140.13, 135.76, 135.30, 131.68, 128.68, 126.10, 124.13, 118.77, 117.73, 115.83, 107.35, 104.52, 99.24, 90.95, 54.31×2, 49.69×2, 44.85, 31.46. ESI-MS *m/z*: 507.1 (M + H)<sup>+</sup>, calcd for C<sub>24</sub>H<sub>27</sub>BrN<sub>8</sub>: 506.15.

#### 4.1.6.5.

*N*<sup>2</sup>-(5-amino-2-methoxy-4-(4-methylpiperazin-1-yl)phenyl)-5-bromo-*N*<sup>4</sup>-(1-methyl-1*H*-indol-6-yl)pyrimidine-2,4-diamine (**18e**). White powder, 65.3 % yield. <sup>1</sup>H NMR (600 MHz, DMSO-*d*<sub>6</sub>) δ (ppm): 8.553 (s, 1H, -NH-), 8.111 (s, 1H, -NH-), 7.652 (s, 1H, H-6), 7.542 (s, 1H, Ar-H), 7.513 (d, *J* = 8.4 Hz, 1H, Ar-H), 7.295 (t, *J* = 3.0 Hz, 1H, indole-H-2), 7.207 (d, *J* = 8.4 Hz, 1H, Ar-H), 7.198 (s, 1H, Ar-H), 6.602 (s, 1H, Ar-H), 6.405 (t, *J* = 3.0 Hz, 1H, indole-H-3), 3.728 (s, 2H, -NH<sub>2</sub>), 3.700 (s, 3H, -OCH<sub>3</sub>), 3.676 (s, 3H, indole-N-CH<sub>3</sub>), 2.744 (t, *J* = 4.2 Hz, 4H, piperazine-H×4), 2.449 (t, *J* = 4.2 Hz, 4H, piperazine-H×4), 2.220 (s, 3H, N-CH<sub>3</sub>). <sup>13</sup>C NMR (150 MHz, DMSO-*d*<sub>6</sub>) δ 158.28, 157.12, 156.93, 141.26, 136.23, 135.94, 135.23, 132.68,

129.79, 125.06, 124.82, 119.78, 116.87, 107.92, 105.27, 104.14, 100.23, 92.43, 56.45, 55.28×2, 50.39×2, 45.88, 32.38. ESI-MS  $m/z$ : 537.2 (M + H)<sup>+</sup>, calcd for C<sub>25</sub>H<sub>29</sub>BrN<sub>8</sub>O: 536.16.

#### 4.1.6.6.

*N*<sup>4</sup>-(5-bromo-4-((2,3-dihydro-1*H*-inden-5-yl)amino)pyrimidin-2-yl)-*N*<sup>1</sup>-(2-(dimethylamino)ethyl)-*N*<sup>1</sup>-methylbenzene-1,2,4-triamine (**18f**). White powder, 83.6 % yield. <sup>1</sup>H NMR (600 MHz, DMSO-*d*<sub>6</sub>)  $\delta$  (ppm): 8.912 (s, 1H, -NH-), 8.328 (s, 1H, -NH-), 8.109 (s, 1H, H-6), 7.511 (s, 1H, Ar-H), 7.311 (d, *J* = 8.4 Hz, 1H, Ar-H), 7.183 (d, *J* = 8.4 Hz, 1H, Ar-H), 6.791 (s, 1H, Ar-H), 6.784 (d, *J* = 9.0 Hz, 1H, Ar-H), 6.713 (d, *J* = 8.4 Hz, 1H, Ar-H), 4.718 (s, 2H, -NH<sub>2</sub>), 2.853 (t, *J* = 7.2 Hz, 2H, -CH<sub>2</sub>-CH<sub>2</sub>-N(CH<sub>3</sub>)<sub>2</sub>), 2.841 (t, *J* = 7.2 Hz, 2H, 2,3-dihydro-indene-CH<sub>2</sub>), 2.775 (t, *J* = 7.2 Hz, 2H, 2,3-dihydro-indene-CH<sub>2</sub>), 2.532 (s, 3H, N-CH<sub>3</sub>), 2.301 (t, *J* = 7.2 Hz, 2H, -CH<sub>2</sub>-CH<sub>2</sub>-N(CH<sub>3</sub>)<sub>2</sub>), 2.148 (s, 6H, -N(CH<sub>3</sub>)<sub>2</sub>), 2.009-2.058 (m, 2H, 2,3-dihydro-indene-CH<sub>2</sub>). <sup>13</sup>C NMR (150 MHz, DMSO-*d*<sub>6</sub>)  $\delta$  158.37, 157.11, 156.60, 143.81, 142.94, 139.14, 136.88, 136.49, 133.20, 123.80, 121.51, 119.84, 119.65, 108.39, 105.93, 91.89, 57.29, 54.11, 45.65×2, 41.61, 32.49, 31.84, 25.29. ESI-MS  $m/z$ : 496.3 (M + H)<sup>+</sup>, calcd for C<sub>24</sub>H<sub>30</sub>BrN<sub>7</sub>: 495.17.

#### 4.1.6.7.

*N*<sup>2</sup>-(3-amino-4-(4-methylpiperazin-1-yl)phenyl)-5-bromo-*N*<sup>4</sup>-(2,3-dihydro-1*H*-inden-5-yl)pyrimidine-2,4-diamine (**18g**). White powder, 77.3 % yield. <sup>1</sup>H NMR (600 MHz, DMSO-*d*<sub>6</sub>)  $\delta$  (ppm): 8.931 (s, 1H, -NH-), 8.335 (s, 1H, -NH-), 8.110 (s, 1H, H-6), 7.501 (s, 1H, Ar-H), 7.306 (d, *J* = 7.8 Hz, 1H, Ar-H), 7.185 (d, *J* = 7.8 Hz, 1H, Ar-H),

6.839-6.822 (m, 2H, Ar-H), 6.680 (d,  $J = 8.4$  Hz, 1H, Ar-H), 4.486 (s, 2H, -NH<sub>2</sub>), 2.851 (t,  $J = 7.2$  Hz, 4H, 2,3-dihydro-indene-CH<sub>2</sub>×2), 2.727 (t,  $J = 4.2$  Hz, 4H, piperazine-H×4), 2.456 (t,  $J = 4.2$  Hz, 4H, piperazine-H×4), 2.217 (s, 3H, N-CH<sub>3</sub>), 2.016-2.064 (m, 2H, 2,3-dihydro-indene-CH<sub>2</sub>). <sup>13</sup>C NMR (150 MHz, DMSO)  $\delta$  158.35, 157.09, 156.61, 143.81, 142.01, 139.20, 136.85, 136.57, 132.91, 123.80, 121.51, 119.68, 118.74, 108.65, 106.00, 91.95, 55.33×2, 50.73×2, 45.87, 32.49, 31.86, 25.31. ESI-MS  $m/z$ : 494.2 (M + H)<sup>+</sup>, calcd for C<sub>24</sub>H<sub>28</sub>BrN<sub>7</sub>: 493.15.

#### 4.1.6.8.

*N*<sup>2</sup>-(5-amino-2-methoxy-4-(4-methylpiperazin-1-yl)phenyl)-5-bromo-*N*<sup>4</sup>-(2,3-dihydro-1*H*-inden-5-yl)pyrimidine-2,4-diamine (**18h**). White powder, 66.5 % yield. <sup>1</sup>H NMR (600 MHz, DMSO-*d*<sub>6</sub>)  $\delta$  (ppm): 8.335 (s, 1H, -NH-), 8.095 (s, 1H, -NH-), 7.675 (s, 1H, H-6), 7.427 (s, 1H, Ar-H), 7.311 (d,  $J = 8.4$  Hz, 1H, Ar-H), 7.157 (d,  $J = 7.8$  Hz, 1H, Ar-H), 7.125 (s, 1H, Ar-H), 6.630 (s, 1H, Ar-H), 4.061 (s, 2H, -NH<sub>2</sub>), 3.682 (s, 3H, -OCH<sub>3</sub>), 2.819 (t,  $J = 7.2$  Hz, 4H, 2,3-dihydro-indene-CH<sub>2</sub>×2), 2.797 (t,  $J = 4.2$  Hz, 4H, piperazine-H×4), 2.473 (t,  $J = 4.2$  Hz, 4H, piperazine-H×4), 2.228 (s, 3H, N-CH<sub>3</sub>), 1.983-2.033 (m, 2H, 2,3-dihydro-indene-CH<sub>2</sub>). <sup>13</sup>C NMR (150 MHz, DMSO)  $\delta$  158.61, 157.11, 156.60, 143.86, 142.15, 139.08, 136.84, 135.33, 133.40, 124.49, 123.78, 121.33, 119.20, 109.33, 104.13, 92.31, 56.32, 55.29×2, 50.38×2, 45.91, 32.45, 31.80, 25.17. ESI-MS  $m/z$ : 524.2 (M + H)<sup>+</sup>, calcd for C<sub>25</sub>H<sub>30</sub>BrN<sub>7</sub>O: 523.16.

#### 4.1.6.9.

*N*<sup>2</sup>-(5-amino-2-methoxy-4-(4-methylpiperazin-1-yl)phenyl)-*N*<sup>4</sup>-(1-methyl-1*H*-indol-6-yl)pyrimidine-2,4-diamine (**18i**). White powder, 72.9 % yield. <sup>1</sup>H NMR (600 MHz,

DMSO- $d_6$ )  $\delta$  (ppm): 9.222 (s, 1H, -NH-), 7.925 (d,  $J = 6.0$  Hz, 1H, H-6), 7.797 (s, 1H, -NH-), 7.586 (s, 1H, Ar-H), 7.467 (d,  $J = 8.4$  Hz, 1H, Ar-H), 7.403 (s, 1H, Ar-H), 7.232 (t,  $J = 3.0$  Hz, 1H, indole-H-2), 7.107 (d,  $J = 8.4$  Hz, 1H, Ar-H), 6.655 (s, 1H, Ar-H), 6.356 (d,  $J = 2.4$  Hz, 1H, indole-H-3), 6.184 (d,  $J = 6.0$  Hz, 1H, H-5), 4.146 (s, 2H, -NH<sub>2</sub>), 3.736 (s, 3H, -OCH<sub>3</sub>), 3.684 (s, 3H, indole-N-CH<sub>3</sub>), 2.798 (t,  $J = 4.2$  Hz, 4H, piperazine-H $\times$ 4), 2.476 (t,  $J = 4.2$  Hz, 4H, piperazine-H $\times$ 4), 2.233 (s, 3H, N-CH<sub>3</sub>). <sup>13</sup>C NMR (150 MHz, DMSO)  $\delta$  160.98, 159.67, 155.75, 140.98, 136.55, 135.56, 134.01, 132.29, 129.16, 125.50, 123.96, 120.22, 114.14, 107.96, 104.16, 101.83, 100.20, 97.86, 56.56, 55.34 $\times$ 2, 50.49 $\times$ 2, 45.91, 32.26. ESI-MS  $m/z$ : 461.2 (M + H)<sup>+</sup>, calcd for C<sub>25</sub>H<sub>30</sub>N<sub>8</sub>O: 458.25.

#### 4.1.7. General procedure for the preparation of target compounds **19a-19i**

Acryloyl chloride (0.2 mmol in THF) was added dropwise to the solution of **18a-18i** (100 mg, 0.2 mmol) and DIPEA (0.04 mL, 0.2 mmol) in THF (10 mL) at -60 °C under nitrogen. The resulting suspension was stirred at -60 °C for 1 h, then warm to room temperature for 3h, dissolved in ethyl acetate (20 mL), and washed with water and saturated brine. The organic layer was evaporated and purified by flash silica chromatography with an elution gradient of 5% MeOH/TEA in ethyl acetate. Pure fractions were evaporated and dried to give target compounds.

##### 4.1.7.1.

*N*-(5-((4-((1*H*-indol-6-yl)amino)-5-bromopyrimidin-2-yl)amino)-2-((2-(dimethylamino)ethyl)(methyl)amino)phenyl)acrylamide (**19a**). White powder, 44.5 % yield. m.p: 190.1-192.6 °C. <sup>1</sup>H NMR (600 MHz, DMSO- $d_6$ )  $\delta$  (ppm): 11.027 (s, 1H, indole-H-1),

10.129 (s, 1H, -NH-), 9.132 (s, 1H, -NH-), 8.510 (s, 1H, -NH-), 8.232 (s, 1H, Ar-H), 8.232 (s, 1H, H-6), 7.516 (s, 1H, Ar-H), 7.470 (d,  $J = 8.4$  Hz, 1H, Ar-H), 7.414 (d,  $J = 9.0$  Hz, 1H, Ar-H), 7.309 (t,  $J = 3.0$  Hz, 1H, indole-H-2), 7.181 (d,  $J = 8.4$  Hz, 1H, Ar-H), 6.826 (d,  $J = 7.8$  Hz, 1H, Ar-H), 6.400 (t,  $J = 2.4$  Hz, 1H, indole-H-3), 6.353 (dd,  $J_1 = 17.0$  Hz,  $J_2 = 10.2$  Hz, 1H, -CH=CH<sub>2</sub>), 6.226 (d,  $J = 16.8$  Hz, 1H, -CH=CH<sub>2</sub>), 5.950 (d,  $J = 12.0$  Hz, 1H, -CH=CH<sub>2</sub>), 2.720 (t,  $J = 7.2$  Hz, 2H, -CH<sub>2</sub>-CH<sub>2</sub>-N(CH<sub>3</sub>)<sub>2</sub>), 2.569 (s, 3H, N-CH<sub>3</sub>), 2.207 (t,  $J = 7.2$  Hz, 2H, -CH<sub>2</sub>-CH<sub>2</sub>-N(CH<sub>3</sub>)<sub>2</sub>), 2.171 (s, 6H, -N(CH<sub>3</sub>)<sub>2</sub>). <sup>13</sup>C NMR (150 MHz, DMSO-*d*<sub>6</sub>)  $\delta$  162.57, 158.32, 157.22, 156.91, 136.99, 136.52, 135.78, 134.34, 132.23, 132.14, 126.45, 125.30, 125.00, 121.49, 119.28, 117.08, 115.65, 111.87, 107.60, 100.86, 92.56, 56.83, 56.01, 45.17 $\times$ 2, 42.61. ESI-MS  $m/z$ : 549.2 (M + H)<sup>+</sup>, calcd for C<sub>26</sub>H<sub>29</sub>BrN<sub>8</sub>O: 548.16.

#### 4.1.7.2.

*N*-(5-((4-((1*H*-indol-6-yl)amino)-5-bromopyrimidin-2-yl)amino)-2-(4-methylpiperazin-1-yl)phenyl)acrylamide (**19b**). White powder, 56.8 % yield. m.p: 145.2-146.7 °C. <sup>1</sup>H NMR (600 MHz, DMSO-*d*<sub>6</sub>)  $\delta$  (ppm): 11.054 (s, 1H, indole-H-1), 9.150 (s, 1H, -NH-), 8.954 (s, 1H, -NH-), 8.532 (s, 1H, -NH-), 8.137 (s, 1H, H-6), 7.984 (s, 1H, Ar-H), 7.533 (s, 1H, Ar-H), 7.502 (d,  $J = 8.4$  Hz, 1H, Ar-H), 7.478 (d,  $J = 9.0$  Hz, 1H, Ar-H), 7.329 (t,  $J = 2.4$  Hz, 1H, indole-H-2), 7.169 (d,  $J = 8.4$  Hz, 1H), 6.689 (d,  $J = 5.4$  Hz, 1H, Ar-H), 6.571 (dd,  $J_1 = 17.0$  Hz,  $J_2 = 10.2$  Hz, 1H, -CH=CH<sub>2</sub>), 6.432 (t,  $J = 2.4$  Hz, 1H, indole-H-3), 6.209 (d,  $J = 17.4$  Hz, 1H, -CH=CH<sub>2</sub>), 5.734 (d,  $J = 10.2$  Hz, 1H, -CH=CH<sub>2</sub>), 2.694 (t,  $J = 4.8$  Hz, 4H, piperazine-H $\times$ 4), 2.510 (t,  $J = 4.8$  Hz,



4H, piperazine-H $\times$ 4), 2.246 (s, 3H, N-CH<sub>3</sub>). <sup>13</sup>C NMR (150 MHz, DMSO-*d*<sub>6</sub>)  $\delta$  162.83, 158.27, 157.28, 156.89, 137.34, 136.50, 135.80, 132.31, 132.23, 131.81, 126.37, 125.33, 125.07, 119.45, 119.39, 117.09, 115.98, 113.43, 107.75, 100.93, 92.55, 54.88 $\times$ 2, 51.51 $\times$ 2, 45.73. ESI-MS *m/z*: 547.0 (M + H)<sup>+</sup>, calcd for C<sub>26</sub>H<sub>27</sub>BrN<sub>8</sub>O: 546.14.

#### 4.1.7.3.

*N*-(5-((4-((1*H*-indol-6-yl)amino)-5-bromopyrimidin-2-yl)amino)-4-methoxy-2-(4-methylpiperazin-1-yl)phenyl)acrylamide (**19c**). White powder, 68.5 % yield. m.p: 158.9-160.2 °C. <sup>1</sup>H NMR (600 MHz, DMSO-*d*<sub>6</sub>)  $\delta$  (ppm): 10.958 (s, 1H, indole-H-1), 8.948 (s, 1H, -NH-), 8.396 (s, 1H, -NH-), 8.240 (s, 1H, -NH-), 8.113 (s, 1H, H-6), 7.730 (s, 1H, Ar-H), 7.524 (s, 1H, Ar-H), 7.398 (d, *J* = 8.4 Hz, 1H, Ar-H), 7.276 (t, *J* = 2.4 Hz, 1H, indole-H-2), 7.208 (d, *J* = 8.4 Hz, 1H, Ar-H), 6.779 (s, 1H, Ar-H), 6.779 (dd, *J* 1= 16.8 Hz, *J* 2= 10.2 Hz, 1H, -CH=CH<sub>2</sub>), 6.352 (t, *J* = 2.4 Hz, 1H, indole-H-3), 6.188 (d, *J* = 16.8 Hz, 1H, -CH=CH<sub>2</sub>), 5.714 (d, *J* = 10.2 Hz, 1H, -CH=CH<sub>2</sub>), 3.778 (s, 3H, -OCH<sub>3</sub>), 2.888 (t, *J* = 4.8 Hz, 4H, piperazine-H $\times$ 4), 2.505 (t, *J* = 4.8 Hz, 4H, piperazine-H $\times$ 4), 2.399 (s, 3H, N-CH<sub>3</sub>). <sup>13</sup>C NMR (150 MHz, DMSO-*d*<sub>6</sub>)  $\delta$  162.96, 160.60, 158.63, 156.77, 137.99, 136.97, 135.65, 132.28, 125.98, 125.17, 124.56, 119.26, 118.13, 116.08, 113.04, 111.16, 107.11, 106.04, 103.49, 100.91, 98.37, 55.86, 54.24 $\times$ 2, 48.56 $\times$ 2, 45.52. ESI-MS *m/z*: 577.1 (M + H)<sup>+</sup>, calcd for C<sub>27</sub>H<sub>29</sub>BrN<sub>8</sub>O<sub>2</sub>: 576.16.

#### 4.1.7.4.

*N*-(5-((5-bromo-4-((1-methyl-1*H*-indol-6-yl)amino)pyrimidin-2-yl)amino)-2-(4-methyl

*piperazin-1-yl)phenyl)acrylamide (19d)*. White powder, 72.8 % yield. m.p: 133.1-137.4 °C. <sup>1</sup>H NMR (500 MHz, DMSO-*d*<sub>6</sub>) δ (ppm): 9.203 (s, 1H, -NH-), 8.957 (s, 1H, -NH-), 8.544 (s, 1H, -NH-), 8.151 (s, 1H, H-6), 7.984 (s, 1H, Ar-H), 7.651 (s, 1H, Ar-H), 7.494 (d, *J* = 8.5 Hz, 1H, Ar-H), 7.466 (d, *J* = 9.0 Hz, 1H, Ar-H), 7.309 (d, *J* = 2.5 Hz, 1H, indole-H-2), 7.207 (d, *J* = 8.5 Hz, 1H, Ar-H), 6.651 (s, 1H, Ar-H), 6.568 (dd, *J* 1= 17.0 Hz, *J* 2= 10.5 Hz, 1H, -CH=CH<sub>2</sub>), 6.414 (d, *J* = 3.0 Hz, 1H, indole-H-3), 6.199 (d, *J* = 17.0 Hz, 1H, -CH=CH<sub>2</sub>), 5.734 (d, *J* = 10.5 Hz, 1H, -CH=CH<sub>2</sub>), 3.702 (s, 3H, indole-N-CH<sub>3</sub>), 2.689 (t, *J* = 4.0 Hz, 4H, piperazine-H×4), 2.510 (t, *J* = 4.0 Hz, 4H, piperazine-H×4), 2.234 (s, 3H, N-CH<sub>3</sub>). <sup>13</sup>C NMR (125 MHz, DMSO-*d*<sub>6</sub>) δ 162.83, 158.24, 157.06, 156.94, 137.42, 136.49, 136.33, 132.57, 132.29, 131.86, 129.61, 126.38, 125.21, 119.77, 119.27, 116.70, 115.93, 113.57, 105.48, 100.24, 92.59, 54.88×2, 51.54×2, 45.76, 32.47. . ESI-MS *m/z*: 561.3 (M + H)<sup>+</sup>, calcd for C<sub>27</sub>H<sub>29</sub>BrN<sub>8</sub>O: 560.16.

#### 4.1.7.5.

*N*-(5-((5-bromo-4-((1-methyl-1H-indol-6-yl)amino)pyrimidin-2-yl)amino)-4-methoxy-2-(4-methylpiperazin-1-yl)phenyl)acrylamide (**19e**). White powder, 47.3 % yield. m.p: 202.2-204.0 °C. <sup>1</sup>H NMR (600 MHz, DMSO-*d*<sub>6</sub>) δ (ppm): 8.880 (s, 1H, -NH-), 8.391 (s, 1H, -NH-), 8.180 (s, 1H, -NH-), 8.121 (s, 1H, H-6), 7.864 (s, 1H, Ar-H), 7.646 (s, 1H, Ar-H), 7.409 (d, *J* = 8.4 Hz, 1H, Ar-H), 7.273 (d, *J* = 8.4 Hz, 1H, Ar-H), 7.251 (d, *J* = 3.0 Hz, 1H, indole-H-2), 6.778 (s, 1H, Ar-H), 6.571 (dd, *J* 1= 16.8 Hz, *J* 2= 10.2 Hz, 1H, -CH=CH<sub>2</sub>), 6.344 (d, *J* = 3.0 Hz, 1H, indole-H-3), 6.172 (d, *J* = 17.4 Hz, 1H, -CH=CH<sub>2</sub>), 5.706 (d, *J* = 10.8 Hz, 1H, -CH=CH<sub>2</sub>), 3.758 (s, 3H, -OCH<sub>3</sub>), 3.690 (s,

3H, indole-N-CH<sub>3</sub>), 2.822 (t,  $J = 4.2$  Hz, 4H, piperazine-H $\times$ 4), 2.514 (t,  $J = 4.2$  Hz, 4H, piperazine-H $\times$ 4), 2.252 (s, 3H, N-CH<sub>3</sub>). <sup>13</sup>C NMR (150 MHz, DMSO-*d*<sub>6</sub>)  $\delta$  162.85, 158.80, 156.85, 156.59, 148.34, 140.55, 136.21, 132.67, 132.25, 129.45, 125.92, 124.73, 124.28, 123.64, 119.66, 118.66, 115.80, 103.94, 103.45, 100.17, 92.94, 55.80, 54.83 $\times$ 2, 51.19 $\times$ 2, 45.80, 32.37. ESI-MS  $m/z$ : 591.0 (M + H)<sup>+</sup>, calcd for C<sub>28</sub>H<sub>31</sub>BrN<sub>8</sub>O<sub>2</sub>: 590.18.

#### 4.1.7.6.

*N*-(5-((5-bromo-4-((2,3-dihydro-1*H*-inden-5-yl)amino)pyrimidin-2-yl)amino)-2-((2-(*d*imethylamino)ethyl)(methyl)amino)phenyl)acrylamide (**19f**). m.p: 148.7-150.2 °C.

White powder, 62.6 % yield. <sup>1</sup>H NMR (600 MHz, DMSO-*d*<sub>6</sub>)  $\delta$  (ppm): 10.149 (s, 1H, -NH-), 9.214 (s, 1H, -NH-), 8.352 (s, 1H, -NH-), 8.295 (s, 1H, Ar-H), 8.149 (s, 1H, H-6), 7.505 (s, 1H, Ar-H), 7.415 (d,  $J = 8.4$  Hz, 1H, Ar-H), 7.333 (d,  $J = 8.4$  Hz, 1H, Ar-H), 7.135 (d,  $J = 8.4$  Hz, 1H, Ar-H), 7.059 (d,  $J = 9.0$  Hz, 1H, Ar-H), 6.372 (dd,  $J_1 = 16.8$  Hz,  $J_2 = 9.6$  Hz, 1H, -CH=CH<sub>2</sub>), 6.227 (d,  $J = 17.4$  Hz, 1H, -CH=CH<sub>2</sub>), 5.759 (d,  $J = 10.2$  Hz, 1H, -CH=CH<sub>2</sub>), 2.822 (t,  $J = 7.2$  Hz, 2H, -CH<sub>2</sub>-CH<sub>2</sub>-N(CH<sub>3</sub>)<sub>2</sub>), 2.819 (t,  $J = 7.2$  Hz, 2H, 2,3-dihydro-indene-CH<sub>2</sub>), 2.779 (t,  $J = 7.2$  Hz, 2H, 2,3-dihydro-indene-CH<sub>2</sub>), 2.628 (s, 3H, N-CH<sub>3</sub>), 2.250 (t,  $J = 7.2$  Hz, 2H, -CH<sub>2</sub>-CH<sub>2</sub>-N(CH<sub>3</sub>)<sub>2</sub>), 2.186 (s, 6H, -N(CH<sub>3</sub>)<sub>2</sub>), 1.986-2.045 (m, 2H, 2,3-dihydro-indene-CH<sub>2</sub>). <sup>13</sup>C NMR (150 MHz, DMSO-*d*<sub>6</sub>)  $\delta$  162.64, 158.31, 157.19, 156.56, 143.70, 139.10, 136.89, 136.78, 136.72, 134.49, 132.13, 126.54, 123.71, 121.55, 121.30, 119.40, 115.84, 112.28, 92.60, 56.85, 56.01, 45.21 $\times$ 2, 42.58, 32.49, 31.84, 25.29. ESI-MS  $m/z$ : 550.1 (M + H)<sup>+</sup>, calcd for C<sub>27</sub>H<sub>32</sub>BrN<sub>7</sub>O: 549.18.

## 4.1.7.7.

*N*-(5-((5-bromo-4-((2,3-dihydro-1*H*-inden-5-yl)amino)pyrimidin-2-yl)amino)-2-(4-methylpiperazin-1-yl)phenyl)acrylamide (**19g**). White powder, 41.5% yield, m.p: 215.7-217.6 °C. <sup>1</sup>H NMR (600 MHz, DMSO-*d*<sub>6</sub>) δ (ppm): 9.218 (s, 1H, -NH-), 8.994 (s, 1H, -NH-), 8.369 (s, 1H, -NH-), 8.147 (s, 1H, H-6), 8.033 (s, 1H, Ar-H), 7.491 (s, 1H, Ar-H), 7.470 (d, *J* = 8.4 Hz, 1H, Ar-H), 7.320 (d, *J* = 7.8 Hz, 1H, Ar-H), 7.160 (d, *J* = 7.8 Hz, 1H, Ar-H), 6.926 (d, *J* = 8.4 Hz, 1H, Ar-H), 6.588 (dd, *J*<sub>1</sub> = 16.2 Hz, *J*<sub>2</sub> = 10.8 Hz, 1H, -CH=CH<sub>2</sub>), 6.207 (d, *J* = 16.8 Hz, 1H, -CH=CH<sub>2</sub>), 5.743 (d, *J* = 10.2 Hz, 1H, -CH=CH<sub>2</sub>), 2.844 (t, *J* = 7.2 Hz, 2H, 2,3-dihydro-indene-CH<sub>2</sub>), 2.832 (t, *J* = 7.2 Hz, 2H, 2,3-dihydro-indene-CH<sub>2</sub>), 2.747 (t, *J* = 4.8 Hz, 4H, piperazine-H×4), 2.502 (t, *J* = 4.8 Hz, 4H, piperazine-H×4), 2.238 (s, 3H, N-CH<sub>3</sub>), 2.013-2.062 (m, 2H, 2,3-dihydro-indene-CH<sub>2</sub>). <sup>13</sup>C NMR (150 MHz, DMSO-*d*<sub>6</sub>) δ 162.85, 158.24, 157.16, 156.61, 143.70, 139.19, 137.58, 136.72, 136.37, 132.30, 131.97, 126.42, 123.80, 121.36, 119.52, 119.45, 116.15, 113.82, 92.58, 54.89×2, 51.59×2, 45.77, 32.51, 31.87, 25.32. ESI-MS *m/z*: 548.2 (M + H)<sup>+</sup>, calcd for C<sub>27</sub>H<sub>30</sub>BrN<sub>7</sub>O: 547.17.

## 4.1.7.8.

*N*-(5-((5-bromo-4-((2,3-dihydro-1*H*-inden-5-yl)amino)pyrimidin-2-yl)amino)-4-methoxy-2-(4-methylpiperazin-1-yl)phenyl)acrylamide (**19h**). White powder, 65.0% yield, m.p: 156.7-157.9 °C. <sup>1</sup>H NMR (600 MHz, DMSO-*d*<sub>6</sub>) δ (ppm): 8.903 (s, 1H, -NH-), 8.218 (s, 1H, -NH-), 8.125 (s, 1H, -NH-), 8.105 (s, 1H, H-6), 7.964 (s, 1H, Ar-H), 7.409 (s, 1H, Ar-H), 7.338 (d, *J* = 7.8 Hz, 1H, Ar-H), 7.055 (d, *J* = 7.8 Hz, 1H, Ar-H), 6.804 (s, 1H, Ar-H), 6.583 (dd, *J*<sub>1</sub> = 16.8 Hz, *J*<sub>2</sub> = 10.2 Hz, 1H, -CH=CH<sub>2</sub>), 6.163 (d,

$J = 16.8$  Hz, 1H,  $-\text{CH}=\underline{\text{CH}_2}$ ), 5.702 (d,  $J = 10.2$  Hz, 1H,  $-\text{CH}=\underline{\text{CH}_2}$ ), 3.769 (s, 3H,  $-\text{OCH}_3$ ), 2.835 (t,  $J = 4.8$  Hz, 4H, piperazine-H $\times$ 4), 2.775 (t,  $J = 7.2$  Hz, 2H, 2,3-dihydro-indene- $\text{CH}_2$ ), 2.763 (t,  $J = 7.2$  Hz, 2H, 2,3-dihydro-indene- $\text{CH}_2$ ), 2.521 (t,  $J = 4.8$  Hz, 4H, piperazine-H $\times$ 4), 2.246 (s, 3H, N- $\text{CH}_3$ ), 1.953-2.001 (m, 2H, 2,3-dihydro-indene- $\text{CH}_2$ ).  $^{13}\text{C}$  NMR (150 MHz, DMSO- $d_6$ )  $\delta$  162.85, 158.92, 157.16, 156.28, 148.68, 143.63, 140.70, 138.64, 136.73, 132.28, 125.99, 124.34, 123.69, 123.50, 120.38, 118.95, 118.26, 103.49, 92.70, 55.76, 54.84 $\times$ 2, 51.23 $\times$ 2, 45.81, 32.51, 31.79, 25.13. ESI-MS  $m/z$ : 578.1 (M + H) $^+$ , calcd for  $\text{C}_{28}\text{H}_{32}\text{BrN}_7\text{O}_2$ : 577.18.

#### 4.1.7.9.

*N*-(4-methoxy-5-((4-((1-methyl-1H-indol-6-yl)amino)pyrimidin-2-yl)amino)-2-(4-methylpiperazin-1-yl)phenyl)acrylamide (**19i**). White powder, 41.5% yield, m.p: 104.1-106.3 °C.  $^1\text{H}$  NMR (500 MHz, DMSO- $d_6$ )  $\delta$  (ppm): 9.236 (s, 1H, -NH-), 8.955 (s, 1H, -NH-), 8.433 (s, 1H, -NH-), 7.916 (d,  $J = 5.5$  Hz, 1H, H-6), 7.740 (s, 1H, Ar-H), 7.628 (s, 1H, Ar-H), 7.422 (d,  $J = 8.5$  Hz, 1H, Ar-H), 7.212 (d,  $J = 2.0$  Hz, 1H, indole-H-2), 7.180 (d,  $J = 9.0$  Hz, 1H, Ar-H), 6.816 (s, 1H, Ar-H), 6.579 (dd,  $J$  1= 17.0 Hz,  $J$  2= 10.5 Hz, 1H), 6.324 (d,  $J = 2.5$  Hz, 1H, indole-H-3), 6.192 (s, 1H, Ar-H), 6.163 (d,  $J = 17.5$  Hz, 1H,  $-\text{CH}=\underline{\text{CH}_2}$ ), 5.694 (d,  $J = 10.0$  Hz, 1H,  $-\text{CH}=\underline{\text{CH}_2}$ ), 3.829 (s, 3H,  $-\text{OCH}_3$ ), 3.681 (s, 3H, indole-N- $\text{CH}_3$ ), 2.843 (t,  $J = 4.0$  Hz, 4H, piperazine-H $\times$ 4), 2.546 (t,  $J = 4.0$  Hz, 4H, piperazine-H $\times$ 4), 2.267 (s, 3H, N- $\text{CH}_3$ ).  $^{13}\text{C}$  NMR (125 MHz, DMSO- $d_6$ )  $\delta$  162.86, 160.93, 159.831, 155.57, 147.33, 139.646, 136.53, 134.15, 132.26, 129.01, 125.92, 124.466, 124.39, 123.785, 120.19, 117.60, 113.79, 103.32, 101.248, 100.17, 98.365, 55.96, 54.84 $\times$ 2, 51.19 $\times$ 2, 45.72, 32.31.

ESI-MS  $m/z$ : 513.3 (M + H)<sup>+</sup>, calcd for C<sub>28</sub>H<sub>32</sub>N<sub>8</sub>O<sub>2</sub>: 512.26.

#### 4.1.8. Synthesis of 4-fluoro-2-methoxy-5-nitroaniline (**20b**)

4-Fluoro-2-methoxyaniline (1.4 g, 10 mmol) was added portion-wise to concentrated H<sub>2</sub>SO<sub>4</sub> (10 mL) in ice-water bath. After the solid dissolved, concentrated nitric acid (10 mmol) was added portion-wise, stirred overnight and poured into cooled water. The mixture was basified by NH<sub>4</sub>OH, the solid was filtered off and dissolved in ethyl acetate, washed with water and purified by silica chromatography to afford **20b** (1.3 g, 70%) as a yellow crystalline solid. <sup>1</sup>H NMR (600 MHz, DMSO-*d*<sub>6</sub>)  $\delta$  (ppm): 7.337 (d,  $J$  = 7.8 Hz, 1H, Ar-H), 7.028 (d,  $J$  = 13.8 Hz, 1H, Ar-H), 5.233 (s, 2H, -NH<sub>2</sub>), 3.902 (s, 3H, -OCH<sub>3</sub>). ESI-MS  $m/z$ : 187.3 (M + H)<sup>+</sup>, calcd for C<sub>7</sub>H<sub>7</sub>FN<sub>2</sub>O<sub>3</sub>: 186.04.

#### 4.2 Molecular docking study

The binding pose of compounds in the ATP-binding site of EGFR was predicted by the Glide [37] module in Schrodinger (Schrödinger, Inc.). The crystal structures of EGFR<sup>T790M</sup> and EGFR<sup>WT</sup> were downloaded from the Protein Data Bank (PDB code: 3IKA and 4WKQ, respectively) and prepared by using the Protein Preparation Wizard in Maestro (Schrödinger, Inc.), including removing all non-bonded hetero-atoms and water molecules, adding missing hydrogen atoms, and optimizing the structure to relieve steric clashes using the OPLS2005 force field. The scoring grid for docking was generated by enclosing the residues 25 Å around the ATP-binding site using Receptor Grid Generation (Schrödinger, Inc.) with the default settings. The prepared compounds were then docked using the Glide extra precision (XP) scoring mode.

#### 4.3 Covalent docking study

The binding pose of 19e and 19h in the ATP-binding site of EGFR<sup>T790M</sup> was predicted by the CovDock algorithm [38] (Schrödinger, Inc.), which uses both Glide and Prime. The CovDock algorithm is developed to mimic the covalent ligand binding by first positioning the pre-reaction form of the ligand in the binding site close to the receptor reactive residue using Glide docking with positional constraints and only then, generating the covalent attachment. In the pre-reaction docking step, the crystal structures of EGFR<sup>T790M</sup> were downloaded from the Protein Data Bank (PDB code: 3IKA) and prepared by using the Protein Preparation Wizard in Maestro (Schrödinger, Inc.), including removing all non-bonded hetero-atoms and water molecules, adding missing hydrogen atoms, and optimizing the structure to relieve steric clashes using the OPLS2005 force field. Michael addition was used as reaction type and Cys797 was defined as the reactive residue. In the docking step, a large number of potential poses were generated. The optimal pose, based on its Prime energy property was selected for further analysis.

#### 4.4 *In vitro* enzymatic activity assay [28]

Kinases domains of wild-type EGFR (EGFR<sup>WT</sup>) and dual-mutant EGFR (EGFR<sup>L858R/T790M</sup>) were expressed using the Bac-to-Bac baculovirus expression system (Invitrogen, Carlsbad, CA, USA) and purified in Ni-NTA columns (QIAGEN Inc., Valencia, CA, USA). The kinase activity was determined with enzyme-linked immunosorbent assay (ELISA).

#### 4.5 Inhibition of cell proliferation assay

NCI-H1975 and A431 cells were obtained from the American Type Culture Collection. Cells were seeded in 96-well plates (3000 cells per well) and grown overnight. The cells were treated with different concentrations of the compounds for 72 h. Following treatment, cells were fixed with 10% precooled trichloroacetic acid (TCA) for 2 h at 4 °C and stained for 15 min at room temperature with 100 µL of 4 mg/mL sulforhodamine B (SRB, Sigma) solution in 1% acetic acid. After washing the plates three times, the SRB solution was dissolved in 150 µL of 10 mmol/L Tris base for 5 min. Absorbance was measured at 515 nm using a multiwell spectrophotometer (VERSAmax, Molecular Devices). The percent inhibition rate was calculated as  $[1 - (A_{515 \text{ treated}}/A_{515 \text{ control}})] \times 100$ . The IC<sub>50</sub> value was obtained using the Logit method.

#### 4.6 Western blot analysis

Cells or tumor tissues were homogenized in protein lysis buffer. Cellular debris was removed by centrifugation of samples at 12,000 xg for 10 min at 4 °C. The sample protein concentrations were determined by using the Bradford protein assay kit (Bio-Rad, Hercules, CA). Equivalent amounts of proteins were loaded and separated by 8% SDS-PAGE followed by transfer to nitrocellulose membranes. Western blot analysis was subsequently performed using standard procedures. Antibodies used for detection of proteins were p-EGFR (Y1068; Cell Signaling Technology), EGFR (Cell Signaling Technology), p-ERK (T202/Y204; Cell Signaling Technology), ERK (no. Cell Signaling), tubulin (Cell Signaling), Anti-GAPDH antibody (Cell Signaling).

#### 4.7 Determination of pharmacokinetic parameters in rats



The pharmacokinetic parameters of the compound were conducted at Shanghai Medicilon, Inc. The compound was dissolved in a vehicle of 5% DMSO and 95% hydroxypropyl-beta-cyclodextrin aqueous solution (HP- $\beta$ -CD, 20%). Male Sprague–Dawley rats (190–220 g) were given the test compounds intravenously (iv) at 1 mg/kg and by oral gavage (po) at 10 mg/kg. At time points ranging from 0.083, 0.25, 0.5, 1, 2, 4, 8, and 24 h (iv) or 0.25, 0.5, 1 h, 2 h, 4 h, 6 h, 8 h and 24 h (po) post-treatment, blood samples were collected from each rat and separated by centrifugation (8000  $\times$ g, 6 min). The plasma supernatant samples were analyzed by LC–MS/MS (SIMADZULC system;), and the acquired data were analyzed with WinNonlin Professional v 5.2 (Pharsight, USA).

#### 4.8 Xenograft models

The mouse studies were conducted in compliance with the Wenzhou Medical University's Policy on the Care and Use of Laboratory Animals. Protocols for the mouse studies were approved by the Wenzhou Medical College Animal Policy and Welfare Committee (Approved documents: 2012/ APWC/ 0216). Five-week-old athymic BALB/cA nu/nu female mice (18-20 g) purchased from Vital River Laboratories (Beijing, China) were used for the *in vivo* experiments. The mice were housed at a constant room temperature with a 12/12-hr light/dark cycle and fed a standard rodent diet and given water *ad lib*. H1975 NSCLC cells ( $1 \times 10^6$ ) suspended in 0.1 mL PBS were injected subcutaneously into the right flank of each mouse. Upon attaining an average tumor volume of 100 mm<sup>3</sup> (approximately 18 days post-implantation), the mice were randomized into treatment groups (n = 6 per

group), and injected intraperitoneally (ip) with a water-soluble preparation of the compound in PBS at either 15 or 30 mg/kg. Control mice received liposome vehicle in PBS. The tumor volumes were determined by measuring length (L) and width (W) and calculating volume ( $V = 0.5 \times L \times W^2$ ) at the indicated time points. At the end of study, the mice were sacrificed, and tumors harvested and weighed for used for histological and protein expression analyses.

#### 4.9 Immunohistochemical (IHC) assays and hematoxylin-eosin (H&E) staining

Harvested H1975 tumor tissues were fixed in 10% formalin at room temperature, and processed and embedded in paraffin. Paraffin-embedded tissues were sectioned at 5  $\mu$ m thickness, deparaffinized, rehydrated, and incubated with the primary antibody (ABCAM) at room temperature. Immunoreactivity was detected by 3,3-diaminobenzidine (DAB). For routine histological analysis, the harvested heart, kidney and liver tissues were processed and stained with hematoxylin and eosin (H&E). Each image of the sections was captured using a Nikon microscope (200 $\times$  amplification, Nikon, Japan).

#### 4.10 Kinase Selectivity Profile [39]

The kinase selectivity profile was performed on the DiscoverX KINOMEScan platform (<http://www.kinomescan.com/>). The compounds were screened at 1000 nM. Results of the primary screen are reported as '% Ctrl' (percent of control), where lower numbers indicate stronger hits. “% control” was calculated as follows: % control =  $[(\text{test compound signal} - \text{positive control signal}) / (\text{negative control signal} - \text{positive control signal})] \times 100$ . Negative control = DMSO (100%Ctrl). Positive control =

control compound (0% Ctrl).

### **Acknowledgement**

This study was supported by the National Natural Science Funding of China (81502912, 21472142, and 81622043), and the Natural Science Funding of Zhejiang Province (LY17B020008, LY17H300004 and LQ15H300002).

### **Supplementary data**

Additional experiments, Table S1, Scheme S1-S3 and Figure S1–S3.

### **References**

- [1] Z. Song, Y. Ge, C. Wang, S. Huang, X. Shu, K. Liu, Y. Zhou, X. Ma, Challenges and Perspectives on the Development of Small-Molecule EGFR Inhibitors against T790M-Mediated Resistance in Non-Small-Cell Lung Cancer, *J Med Chem*, 59 (2016) 6580-6594.
- [2] L.A. Torre, F. Bray, R.L. Siegel, J. Ferlay, J. Lortet-Tieulent, A. Jemal, Global cancer statistics, 2012, *CA Cancer J Clin*, 65 (2015) 87-108.
- [3] R.L. Siegel, K.D. Miller, A. Jemal, Cancer Statistics, 2017, *CA Cancer J Clin*, 67 (2017) 7-30.
- [4] S.V. Sharma, D.W. Bell, J. Settleman, D.A. Haber, Epidermal growth factor receptor mutations in lung cancer, *Nat Rev Cancer*, 7 (2007) 169-181.
- [5] F.R. Hirsch, M. Varella-Garcia, P.A. Bunn, Jr., M.V. Di Maria, R. Veve, R.M. Bremmes, A.E. Baron, C. Zeng, W.A. Franklin, Epidermal growth factor receptor in non-small-cell lung carcinomas: correlation between gene copy number and protein expression and impact on prognosis, *J Clin Oncol*, 21 (2003) 3798-3807.
- [6] S. Kobayashi, T.J. Boggon, T. Dayaram, P.A. Janne, O. Kocher, M. Meyerson,

B.E. Johnson, M.J. Eck, D.G. Tenen, B. Halmos, EGFR mutation and resistance of non-small-cell lung cancer to gefitinib, *N Engl J Med*, 352 (2005) 786-792.

[7] J.A. Engelman, P.A. Janne, Mechanisms of acquired resistance to epidermal growth factor receptor tyrosine kinase inhibitors in non-small cell lung cancer, *Clin Cancer Res*, 14 (2008) 2895-2899.

[8] S. Sogabe, Y. Kawakita, S. Igaki, H. Iwata, H. Miki, D.R. Cary, T. Takagi, S. Takagi, Y. Ohta, T. Ishikawa, Structure-Based Approach for the Discovery of Pyrrolo[3,2-d]pyrimidine-Based EGFR T790M/L858R Mutant Inhibitors, *ACS Med Chem Lett*, 4 (2013) 201-205.

[9] J. Stamos, M.X. Sliwkowski, C. Eigenbrot, Structure of the epidermal growth factor receptor kinase domain alone and in complex with a 4-anilinoquinazoline inhibitor, *J Biol Chem*, 277 (2002) 46265-46272.

[10] R.A. Ward, M.J. Anderton, S. Ashton, P.A. Bethel, M. Box, S. Butterworth, N. Colclough, C.G. Chorley, C. Chuaqui, D.A. Cross, L.A. Dakin, J.E. Debreczeni, C. Eberlein, M.R. Finlay, G.B. Hill, M. Grist, T.C. Klinowska, C. Lane, S. Martin, J.P. Orme, P. Smith, F. Wang, M.J. Waring, Structure- and reactivity-based development of covalent inhibitors of the activating and gatekeeper mutant forms of the epidermal growth factor receptor (EGFR), *J Med Chem*, 56 (2013) 7025-7048.

[11] C.H. Yun, K.E. Mengwasser, A.V. Toms, M.S. Woo, H. Greulich, K.K. Wong, M. Meyerson, M.J. Eck, The T790M mutation in EGFR kinase causes drug resistance by increasing the affinity for ATP, *Proc Natl Acad Sci U S A*, 105 (2008) 2070-2075.

[12] D. Marquez-Medina, S. Popat, Afatinib: a second-generation EGF receptor and ErbB tyrosine kinase inhibitor for the treatment of advanced non-small-cell lung cancer, *Future Oncol*, 11 (2015) 2525-2540.

[13] L.V. Sequist, B. Besse, T.J. Lynch, V.A. Miller, K.K. Wong, B. Gitlitz, K. Eaton, C. Zacharchuk, A. Freyman, C. Powell, R. Ananthakrishnan, S. Quinn, J.C. Soria, Neratinib, an irreversible pan-ErbB receptor tyrosine kinase inhibitor: results of a phase II trial in patients with advanced non-small-cell lung cancer, *J Clin Oncol*, 28 (2010) 3076-3083.

[14] T. Mitsudomi, Dacomitinib: another option for EGFR-mutant lung cancer?,

Lancet Oncol, 15 (2014) 1408-1409.

[15] Q. Liu, Y. Sabnis, Z. Zhao, T. Zhang, S.J. Buhrlage, L.H. Jones, N.S. Gray, Developing irreversible inhibitors of the protein kinase cysteinome, *Chem Biol*, 20 (2013) 146-159.

[16] M.L. Sos, H.B. Rode, S. Heynck, M. Peifer, F. Fischer, S. Kluter, V.G. Pawar, C. Reuter, J.M. Heuckmann, J. Weiss, L. Ruddigkeit, M. Rabiller, M. Koker, J.R. Simard, M. Getlik, Y. Yuza, T.H. Chen, H. Greulich, R.K. Thomas, D. Rauh, Chemogenomic profiling provides insights into the limited activity of irreversible EGFR Inhibitors in tumor cells expressing the T790M EGFR resistance mutation, *Cancer Res*, 70 (2010) 868-874.

[17] W. Zhou, D. Ercan, L. Chen, C.H. Yun, D. Li, M. Capelletti, A.B. Cortot, L. Chirieac, R.E. Iacob, R. Padera, J.R. Engen, K.K. Wong, M.J. Eck, N.S. Gray, P.A. Janne, Novel mutant-selective EGFR kinase inhibitors against EGFR T790M, *Nature*, 462 (2009) 1070-1074.

[18] A.O. Walter, R.T. Sjin, H.J. Haringsma, K. Ohashi, J. Sun, K. Lee, A. Dubrovskiy, M. Labenski, Z. Zhu, Z. Wang, M. Sheets, T. St Martin, R. Karp, D. van Kalken, P. Chaturvedi, D. Niu, M. Nacht, R.C. Petter, W. Westlin, K. Lin, S. Jaw-Tsai, M. Raponi, T. Van Dyke, J. Etter, Z. Weaver, W. Pao, J. Singh, A.D. Simmons, T.C. Harding, A. Allen, Discovery of a mutant-selective covalent inhibitor of EGFR that overcomes T790M-mediated resistance in NSCLC, *Cancer Discov*, 3 (2013) 1404-1415.

[19] S. Tomassi, J. Lategahn, J. Engel, M. Keul, H.L. Tumbrink, J. Ketzer, T. Muhlenberg, M. Baumann, C. Schultz-Fademrecht, S. Bauer, D. Rauh, Indazole-Based Covalent Inhibitors To Target Drug-Resistant Epidermal Growth Factor Receptor, *J Med Chem*, (2017).

[20] A.D. Simmons, S. Jaw-Tsai, H.J. Haringsma, A. Allen, T.C. Harding, Insulin-like growth factor 1 (IGF1R)/insulin receptor (INSR) inhibitory activity of rociletinib (CO-1686) and its metabolites in nonclinical models, *Cancer Research*, 75 (2015).

[21] D.A. Cross, S.E. Ashton, S. Ghiorghiu, C. Eberlein, C.A. Nebhan, P.J. Spitzler, J.P. Orme, M.R. Finlay, R.A. Ward, M.J. Mellor, G. Hughes, A. Rahi, V.N. Jacobs, M.

Red Brewer, E. Ichihara, J. Sun, H. Jin, P. Ballard, K. Al-Kadhimi, R. Rowlinson, T. Klinowska, G.H. Richmond, M. Cantarini, D.W. Kim, M.R. Ranson, W. Pao, AZD9291, an irreversible EGFR TKI, overcomes T790M-mediated resistance to EGFR inhibitors in lung cancer, *Cancer Discov*, 4 (2014) 1046-1061.

[22] M.R. Finlay, M. Anderton, S. Ashton, P. Ballard, P.A. Bethel, M.R. Box, R.H. Bradbury, S.J. Brown, S. Butterworth, A. Campbell, C. Chorley, N. Colclough, D.A. Cross, G.S. Currie, M. Grist, L. Hassall, G.B. Hill, D. James, M. James, P. Kemmitt, T. Klinowska, G. Lamont, S.G. Lamont, N. Martin, H.L. McFarland, M.J. Mellor, J.P. Orme, D. Perkins, P. Perkins, G. Richmond, P. Smith, R.A. Ward, M.J. Waring, D. Whittaker, S. Wells, G.L. Wrigley, Discovery of a potent and selective EGFR inhibitor (AZD9291) of both sensitizing and T790M resistance mutations that spares the wild type form of the receptor, *J Med Chem*, 57 (2014) 8249-8267.

[23] G. Lelais, R. Epple, T.H. Marsilje, Y.O. Long, M. McNeill, B. Chen, W. Lu, J. Anumolu, S. Badiger, B. Bursulaya, M. DiDonato, R. Fong, J. Juarez, J. Li, M. Manuia, D.E. Mason, P. Gordon, T. Groessl, K. Johnson, Y. Jia, S. Kasibhatla, C. Li, J. Isbell, G. Spraggon, S. Bender, P.Y. Michellys, Discovery of (R,E)-N-(7-Chloro-1-(1-[4-(dimethylamino)but-2-enoyl]azepan-3-yl)-1H-benzo[d]imidazol-2-yl)-2-methylisonicotinamide (EGF816), a Novel, Potent, and WT Sparing Covalent Inhibitor of Oncogenic (L858R, ex19del) and Resistant (T790M) EGFR Mutants for the Treatment of EGFR Mutant Non-Small-Cell Lung Cancers, *J Med Chem*, 59 (2016) 6671-6689.

[24] S. Chang, L. Zhang, S. Xu, J. Luo, X. Lu, Z. Zhang, T. Xu, Y. Liu, Z. Tu, Y. Xu, X. Ren, M. Geng, J. Ding, D. Pei, K. Ding, Design, synthesis, and biological evaluation of novel conformationally constrained inhibitors targeting epidermal growth factor receptor threonine(7)(9)(0) --> methionine(7)(9)(0) mutant, *J Med Chem*, 55 (2012) 2711-2723.

[25] T. Xu, L. Zhang, S. Xu, C.Y. Yang, J. Luo, F. Ding, X. Lu, Y. Liu, Z. Tu, S. Li, D. Pei, Q. Cai, H. Li, X. Ren, S. Wang, K. Ding, Pyrimido[4,5-d]pyrimidin-4(1H)-one derivatives as selective inhibitors of EGFR threonine790 to methionine790 (T790M) mutants, *Angew Chem Int Ed Engl*, 52 (2013) 8387-8390.

- [26] W. Zhou, X. Liu, Z. Tu, L. Zhang, X. Ku, F. Bai, Z. Zhao, Y. Xu, K. Ding, H. Li, Discovery of pteridin-7(8H)-one-based irreversible inhibitors targeting the epidermal growth factor receptor (EGFR) kinase T790M/L858R mutant, *J Med Chem*, 56 (2013) 7821-7837.
- [27] R.P. Wurz, L.H. Pettus, K. Ashton, J. Brown, J.J. Chen, B. Herberich, F.T. Hong, E. Hu-Harrington, T. Nguyen, D.J. St Jean, Jr., S. Tadesse, D. Bauer, M. Kubryk, J. Zhan, K. Cooke, P. Mitchell, K.L. Andrews, F. Hsieh, D. Hickman, N. Kalyanaraman, T. Wu, D.L. Reid, E.K. Lobenhofer, D.A. Andrews, N. Everds, R. Guzman, A.T. Parsons, S.J. Hedley, J. Tedrow, O.R. Thiel, M. Potter, R. Radinsky, P.J. Beltran, A.S. Tasker, Oxopyrido[2,3-d]pyrimidines as Covalent L858R/T790M Mutant Selective Epidermal Growth Factor Receptor (EGFR) Inhibitors, *ACS Med Chem Lett*, 6 (2015) 987-992.
- [28] Y. Hao, X. Wang, T. Zhang, D. Sun, Y. Tong, Y. Xu, H. Chen, L. Tong, L. Zhu, Z. Zhao, Z. Chen, J. Ding, H. Xie, Y. Xu, H. Li, Discovery and Structural Optimization of N5-Substituted 6,7-Dioxo-6,7-dihydropteridines as Potent and Selective Epidermal Growth Factor Receptor (EGFR) Inhibitors against L858R/T790M Resistance Mutation, *J Med Chem*, 59 (2016) 7111-7124.
- [29] Y. Zhang, L.F. Chen, Q. Zhang, T.Z. Han, F. He, W.Y. Wang, K.L. Pan, Z.G. Liu, G. Liang. The synthesis and antitumor activities and molecular docking of novel pyrimidine EGFR<sup>T790M</sup> inhibitors, *Chinese J Med Chem*, 25 (2015) 269-274. (DOI: 10.14142/j.cnki.cn21-1313/r.2015.04.004)
- [30] J. Yang, L.J. Wang, J.J. Liu, L. Zhong, R.L. Zheng, Y. Xu, P. Ji, C.H. Zhang, W.J. Wang, X.D. Lin, L.L. Li, Y.Q. Wei, S.Y. Yang, Structural optimization and structure-activity relationships of N2-(4-(4-Methylpiperazin-1-yl)phenyl)-N8-phenyl-9H-purine-2,8-diamine derivatives, a new class of reversible kinase inhibitors targeting both EGFR-activating and resistance mutations, *J Med Chem*, 55 (2012) 10685-10699.
- [31] H. Cheng, S.K. Nair, B.W. Murray, C. Almaden, S. Bailey, S. Baxi, D. Behenna, S. Cho-Schultz, D. Dalvie, D.M. Dinh, M.P. Edwards, J.L. Feng, R.A. Ferre, K.S. Gajiwala, M.D. Hemkens, A. Jackson-Fisher, M. Jalaie, T.O. Johnson, R.S. Kania, S.

Kephart, J. Lafontaine, B. Lunney, K.K. Liu, Z. Liu, J. Matthews, A. Nagata, S. Niessen, M.A. Ornelas, S.T. Orr, M. Pairish, S. Planken, S. Ren, D. Richter, K. Ryan, N. Sach, H. Shen, T. Smeal, J. Solowiej, S. Sutton, K. Tran, E. Tseng, W. Vernier, M. Walls, S. Wang, S.L. Weinrich, S. Xin, H. Xu, M.J. Yin, M. Zientek, R. Zhou, J.C. Kath, Discovery of 1-((3R,4R)-3-((5-chloro-2-((1-methyl-1H-pyrazol-4-yl)amino)-7H-pyrrolo[2,3-d]pyrimidin-4-yl)oxy)methyl)-4-methoxypyrrolidin-1-yl)prop-2-en-1-one (PF-06459988), a Potent, WT Sparing, Irreversible Inhibitor of T790M-Containing EGFR Mutants, *J Med Chem*, 59 (2016) 2005-2024.

[32] S. Planken, D.C. Behenna, S.K. Nair, T.O. Johnson, A. Nagata, C. Almaden, S. Bailey, T.E. Ballard, L. Bernier, H. Cheng, S. Cho-Schultz, D. Dalvie, J.G. Deal, D.M. Dinh, M.P. Edwards, R.A. Ferre, K.S. Gajiwala, M.D. Hemkens, R.S. Kania, J.C. Kath, J. Matthews, B.W. Murray, S. Niessen, S.T. Orr, M. Pairish, N.W. Sach, H. Shen, M. Shi, J. Solowiej, K. Tran, E. Tseng, P. Vicini, Y. Wang, S.L. Weinrich, R. Zhou, M. Zientek, L. Liu, Y. Luo, S. Xin, C. Zhang, J.A. Lafontaine, Discovery of N-((3R,4R)-4-fluoro-1-(6-((3-methoxy-1-methyl-1H-pyrazol-4-yl)amino)-9-methyl-9H-purin-2-yl)pyrrolidine-3-yl)acrylamide (PF-06747775) Through Structure-Based Drug Design; A High Affinity Irreversible Inhibitor Targeting Oncogenic EGFR Mutants With Selectivity Over Wild-Type EGFR, *J Med Chem*, (2017).

[33] R.A. Copeland, D.L. Pompliano, T.D. Meek, Drug-target residence time and its implications for lead optimization, *Nat Rev Drug Discov*, 5 (2006) 730-739.

[34] K.S. Thress, C.P. Paweletz, E. Felip, B.C. Cho, D. Stetson, B. Dougherty, Z. Lai, A. Markovets, A. Vivancos, Y. Kuang, D. Ercan, S.E. Matthews, M. Cantarini, J.C. Barrett, P.A. Janne, G.R. Oxnard, Acquired EGFR C797S mutation mediates resistance to AZD9291 in non-small cell lung cancer harboring EGFR T790M, *Nat Med*, 21 (2015) 560-562.

[35] Y. Jia, C.H. Yun, E. Park, D. Ercan, M. Manuia, J. Juarez, C. Xu, K. Rhee, T. Chen, H. Zhang, S. Palakurthi, J. Jang, G. Lelais, M. DiDonato, B. Bursulaya, P.Y. Michellys, R. Epple, T.H. Marsilje, M. McNeill, W. Lu, J. Harris, S. Bender, K.K. Wong, P.A. Janne, M.J. Eck, Overcoming EGFR(T790M) and EGFR(C797S)



resistance with mutant-selective allosteric inhibitors, *Nature*, 534 (2016) 129-132.

[36] D. Yee, Insulin-like growth factor receptor inhibitors: baby or the bathwater?, *J Natl Cancer Inst*, 104 (2012) 975-981.

[37] R.A. Friesner, J.L. Banks, R.B. Murphy, T.A. Halgren, J.J. Klicic, D.T. Mainz, M.P. Repasky, E.H. Knoll, M. Shelley, J.K. Perry, D.E. Shaw, P. Francis, P.S. Shenkin, Glide: a new approach for rapid, accurate docking and scoring. 1. Method and assessment of docking accuracy, *J Med Chem*, 47 (2004) 1739-1749.

[38] D. Toledo Warshaviak, G. Golan, K.W. Borrelli, K. Zhu, O. Kalid, Structure-based virtual screening approach for discovery of covalently bound ligands, *J Chem Inf Model*, 54 (2014) 1941-1950.

[39] M.A. Fabian, W.H. Biggs, 3rd, D.K. Treiber, C.E. Atteridge, M.D. Azimioara, M.G. Benedetti, T.A. Carter, P. Ciceri, P.T. Edeen, M. Floyd, J.M. Ford, M. Galvin, J.L. Gerlach, R.M. Grotzfeld, S. Herrgard, D.E. Insko, M.A. Insko, A.G. Lai, J.M. Lelias, S.A. Mehta, Z.V. Milanov, A.M. Velasco, L.M. Wodicka, H.K. Patel, P.P. Zarrinkar, D.J. Lockhart, A small molecule-kinase interaction map for clinical kinase inhibitors, *Nat Biotechnol*, 23 (2005) 329-336.

### Abbreviations used

EGFR, epidermal growth factor receptor; NSCLC, non-small cell lung cancer; TKI,

tyrosine kinase inhibitor; SAR, structure–activity relationship; INSR, insulin receptor;

IGF1R, insulin-like growth factor 1 receptor; DIPEA, *N,N*-Diisopropylethylamine;

DMF, *N,N*-dimethylformamide; po, per os; iv, intravenous;

Figure 1. Chemical structures of the representative mutant-selective EGFR kinase inhibitors

Figure 2. Modeling studies of **7**

(A) Chemical structure of compound **7** and its depicted binding mode with EGFR<sup>T790M</sup>. (B) 2D interaction diagram of **7** with EGFR<sup>T790M</sup> (PDB code 3IKA). (C) The binding model of compound **7** (purple) bound to EGFR<sup>T790M</sup>. (D) The binding model of compound **7** (purple) bound to EGFR<sup>WT</sup> (PDB code 4G5J).

Figure 3. Structure-based design targeting Cys-797

(A) Compound **15a** (cyan), **15e** (dark blue), and **15f** (purple) in the ATP-binding site (PDB: 3IKA). (B) Chemical structure of compound **15a**, **15e**, **15f**. (C) Distance measurement from the meta-position of the pyrimidine 2-aniline toward the reactive cysteine.

Figure 4. Covalent binding mode of **19e** and **19h**

Panels A and C show the acrylamide group of **19e** and **19h** irreversibly bound to EGFR<sup>T790M</sup> via Cys797. The pyrimidine core forming two hydrogen bonds to the hinge region (Met793), the bromine substituent adjacent to the gatekeeper residue. Panels B and D show the interactions of the methoxy substituent and the pyrimidine 4-substituent with the surrounding hydrophobic amino acid residues.

Figure 5. Effects of **19e** and **19h** on EGFR signaling in H1975 cells and A431 cells. Cells were treated with the indicated concentrations of **19e** and **19h** or compound **3** for 2 h and stimulated by EGF for 15 min. Cell lysates were harvested for Western blot analysis of EGFR and phosphorylated downstream signaling proteins.

Figure 6. Kinase selectivity profile

The kinase selectivity profile of compound **19e** and **19h** against 98 kinases is illustrated with DiscoverX KINOMEScan profiling platform. The compounds were screened at 1000 nM, and results for primary screen binding interactions are reported as '% Ctrl', where lower numbers indicate stronger hits.

Figure 7. Antitumor efficacy of **19e** and **19h** in the H1975 xenograft mouse model. Female BALB/cA nu/nu mice (n = 6) were treated with **19e** (A) and **19h** (B) at 15 and 30 mg/kg/day or vehicle. Tumor volumes were recorded every 2-3 days. (C) Representative photographs of tumors in each group after **19e** and **19h** or vehicle treatment. (D) Comparison of the final tumor weights in each group after the 18-day treatment of **19e** and **19h**. Numbers in columns indicate the mean tumor weight in each group. \*\*p < 0.01, \*\*\*p < 0.001. (E) Western blot analysis of tumor lysates for phosphorylated EGFR (pEGFR). (F) Quantification of pEGFR levels. Data plotted as mean ± SEM. \*\*p < 0.01, \*\*\*p < 0.001 compared to vehicle control. (G) Representative images of immunohistochemical staining for Ki-67 in tumor tissues. Immunoreactivity shown by DAB, brown color.

Table 1. *In vitro* EGFR inhibitory activities of compounds **14a-14h**.<sup>a</sup>

<sup>a</sup>Kinase activity assays were examined by using the ELISA-based EGFR-tyrosine kinase (TK) assay. Data are averages of at least three independent determinations and reported as the mean  $\pm$  SD.

Table 2. *In vitro* EGFR inhibitory activities of compounds **15a-15j**. Data are averages of at least three independent determinations and reported as the mean  $\pm$  SD.

<sup>a</sup>Selectivity ratio = EGFR<sup>WT</sup> IC<sub>50</sub>/ EGFR<sup>L858R/T790M</sup> IC<sub>50</sub>.

Table 3. *In vitro* EGFR inhibition and anti-proliferative activities of compounds **19a-19i**.<sup>a</sup>

<sup>a</sup>The anti-proliferative activities of the compounds were assessed by the sulforhodamine B (SRB) colorimetric assay. Data are averages of at least three independent determinations and reported as the mean  $\pm$  SD.

Table 4. Pharmacokinetic parameters for the representative compounds.

<sup>a</sup>The compound was dissolved in a vehicle of 5% DMSO and 95% hydroxypropyl-beta-cyclodextrin aqueous solution (HP- $\beta$ -CD, 20%). Male Sprague–Dawley rats were administered the test compounds intravenously (iv) at 1 mg/kg and by oral gavage (po) at 10 mg/kg. The plasma supernatant samples were analyzed by LC–MS/MS (SIMADZULC system;), and the acquired data were

analyzed with WinNonlin Professional v 5.2 (Pharsight, USA).

Scheme 1. Synthesis of Compounds **14a-14h**, **15a-15j**.

<sup>a</sup>Reagents and conditions: (a) DIPEA (1.5 equiv), DMF, -60 °C to room temperature, overnight, 60-85%; (b) 1-methylpiperazine (1.5 equiv), K<sub>2</sub>CO<sub>3</sub> (1.0 equiv), DMSO, rt, overnight, 90%; (c) H<sub>2</sub>, 10% Pd/C, MeOH, rt, overnight, 75%; (d) Trifluoroacetic acid, 2-butanol, 100 °C, 3 h; (e) 4,6-dichloro-1H-pyrazolo[3,4-d]pyrimidine, DIPEA (1.5 equiv), DMF; (f) p-TSA, 2-pentanol, 120 °C, 5 h.

Scheme 2. Synthesis of Compounds **19a-19i**.

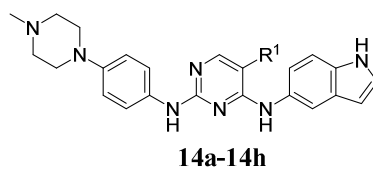
<sup>a</sup>Reagents and conditions: (a) p-TSA (1.0 equiv), 2-pentanol, 120 °C, overnight; (b) 120 °C, 2-pentanol, 2 h; (c) iron (10.0 equiv), NH<sub>4</sub>Cl (1.0 equiv), EtOH, water, 80 °C, 3h; (d) acryloyl chloride (1.0 equiv), DIPEA (1.0 equiv), THF, -60 °C to rt, 4 h; (e) 2,4-dichloropyrimidine (1.0 equiv), DIPEA (1.5 equiv), DMF, -60 °C to rt, overnight.

ACCEPTED MANUSCRIPT

**Table 4**

Compound	route	t <sub>1/2</sub> (h)	C <sub>max</sub> (ng/mL)	AUC <sub>(0-∞)</sub> (h*ng/mL)	Cl (mL/h/kg)	V <sub>ss</sub> (mL/kg)	F (%)
19c	iv	2.88	182	348	2914	7969	
	po	4.46	258	1870	-	-	53.67
19e	iv	3.47	235	515	1954	6558	
	po	3.25	636	2691	-	-	52.30
19h	iv	5.17	407	1052	953	4826	
	po	3.54	452	3742	-	-	35.58
19i	iv	5.86	456	449	2281	8973	
	po	5.31	45	389	-	-	8.68

Table 1



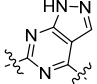
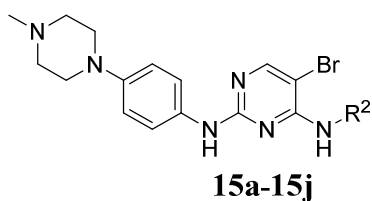
Comp	R <sup>1</sup>	EGFR IC <sub>50</sub> (μM)		
		WT	T790M	L858R/T790M
<b>7</b>	-Cl	0.557 ± 0.120	0.105 ± 0.061	0.046 ± 0.011
<b>14a</b>	-H	0.049 ± 0.013	0.100 ± 0.049	0.220 ± 0.083
<b>14b</b>	-CF <sub>3</sub>	>1.0	0.102 ± 0.052	0.121 ± 0.041
<b>14c</b>	-NO <sub>2</sub>	>1.0	>1.0	0.906 ± 0.546
<b>14d</b>	-OCH <sub>3</sub>	>1.0	0.224 ± 0.032	0.155 ± 0.055
<b>14e</b>	-CH <sub>3</sub>	>1.0	0.197 ± 0.087	0.171 ± 0.090
<b>14f</b>	-F	>1.0	0.232 ± 0.037	0.181 ± 0.084
<b>14g</b>	-Br	>1.0	0.053 ± 0.018	0.035 ± 0.016
<b>14h</b>		0.127 ± 0.050	0.105 ± 0.033	0.140 ± 0.077



Table 2



Comp	R <sup>2</sup>	EGFR IC <sub>50</sub> (μM)		
		WT	L858R/T790M	Selectivity Ratio
<b>14g</b>		0.846 ± 0.094	0.037 ± 0.019	23
<b>15a</b>		1.4 ± 0.27	0.019 ± 0.012	74
<b>15b</b>		0.393 ± 0.025	0.039 ± 0.020	10
<b>15c</b>		1.1 ± 0.27	0.043 ± 0.010	26
<b>15d</b>		0.325 ± 0.20	0.049 ± 0.028	7
<b>15e</b>		1.3 ± 0.369	0.021 ± 0.005	62
<b>15f</b>		6.8 ± 2.5	0.035 ± 0.018	194
<b>15g</b>		14.3 ± 4.4	6.0 ± 0.62	2
<b>15h</b>		5.7 ± 4.3	8.6 ± 3.2	/

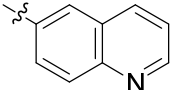
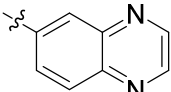
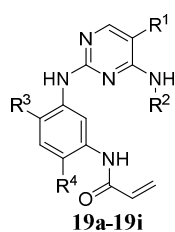
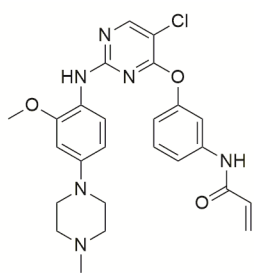
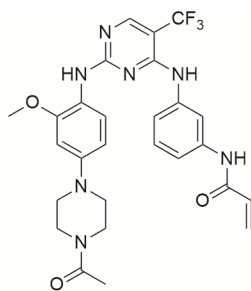
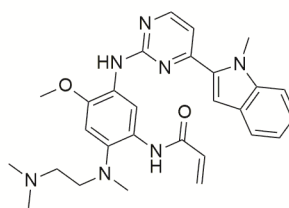
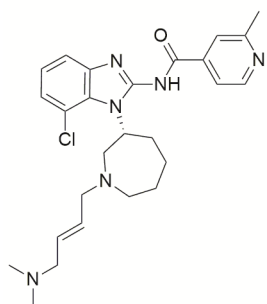
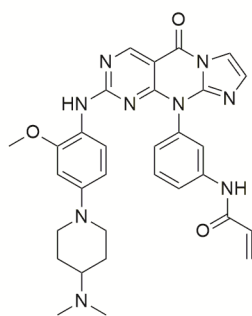
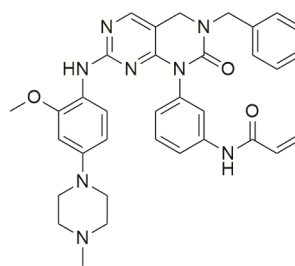
<b>15i</b>		>10.0	$7.8 \pm 3.5$	/
<b>15j</b>		$0.408 \pm 0.405$	$0.236 \pm 0.174$	2
BIBW2992		$0.006 \pm 0.005$	$0.001 \pm 0.001$	6
<b>1</b> (WZ4002)		$0.250 \pm 0.020$	$0.007 \pm 0.001$	35

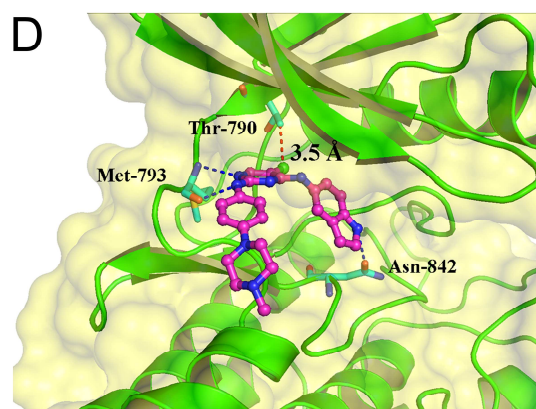
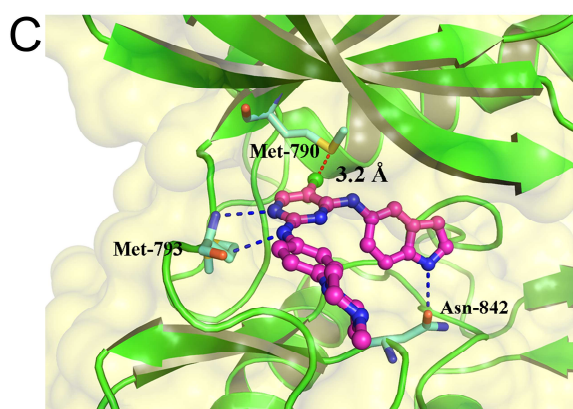
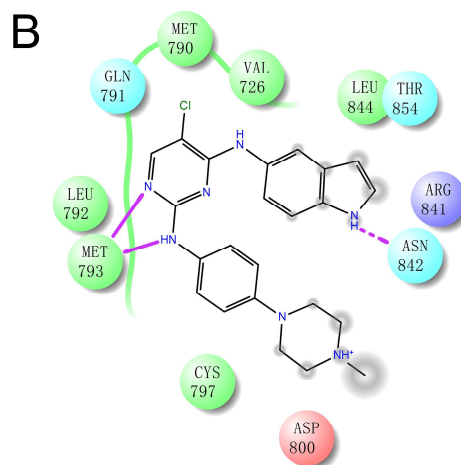
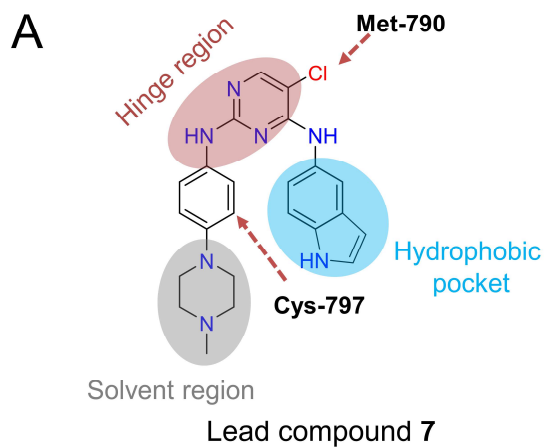
Table 3



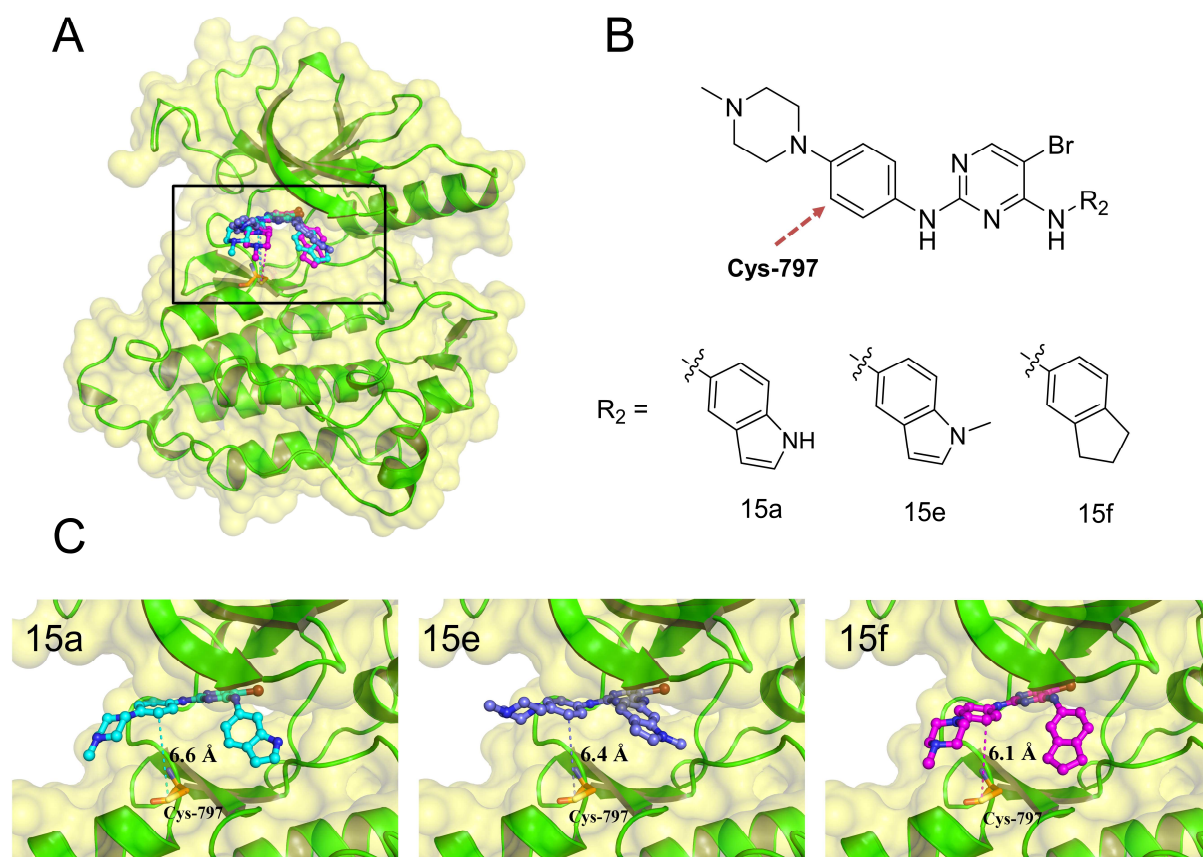
Comp	R <sup>1</sup>	R <sup>2</sup>	R <sup>3</sup>	R <sup>4</sup>	EGFR IC <sub>50</sub> (nM)			Cellular antiproliferative activity (IC <sub>50</sub> , μM)		cLogP <sup>a</sup>
					WT	L858R/ T790M	Selectivity Ratio	A431	H1975	
<b>19a</b>	-Br		-H		8.7 ± 8.2	0.2 ± 0.1	43	0.143 ± 0.096	0.111 ± 0.069	4.57
<b>19b</b>	-Br		-H		233.8 ± 40.1	16.4 ± 11.4	14	0.108 ± 0.065	0.451 ± 0.269	4.32
<b>19c</b>	-Br		-OCH <sub>3</sub>		92.1 ± 28.4	2.7 ± 2.1	34	0.695 ± 0.399	0.132 ± 0.076	4.73
<b>19d</b>	-Br		-H		414.1 ± 286.1	27.8 ± 24.3	15	0.200 ± 0.203	0.190 ± 0.028	4.81
<b>19e</b>	-Br		-OCH <sub>3</sub>		280.4 ± 279.9	4.1 ± 2.4	68	1.693 ± 0.413	0.184 ± 0.108	4.86
<b>19f</b>	-Br		-H		26.2 ± 24.6	0.6 ± 0.6	43	0.256 ± 0.353	0.106 ± 0.055	4.90
<b>19g</b>	-Br		-H		465.7 ± 378.4	27.7 ± 26.4	17	0.135 ± 0.249	0.306 ± 0.203	4.97
<b>19h</b>	-Br		-OCH <sub>3</sub>		202.5 ± 112.4	3.2 ± 1.8	63	2.595 ± 1.847	0.276 ± 0.266	5.23
<b>19i</b>	-H		-OCH <sub>3</sub>		26.9 ± 26.4	8.4 ± 7.1	3	2.091 ± 0.542	0.259 ± 0.132	4.24
BIBW2009					3.7 ± 0.6	9.3 ± 1.9	/	<0.001	0.495 ± 0.371	5.43
<b>1</b> (WZ4002)					223.9 ± 90.6	10.9 ± 3.9	20	1.300 ± 0.218	0.128 ± 0.011	4.54
<b>3</b> (AZD9291)					228.9 ± 140.1	3.3 ± 3.1	69	0.956 ± 0.776	0.064 ± 0.036	4.48

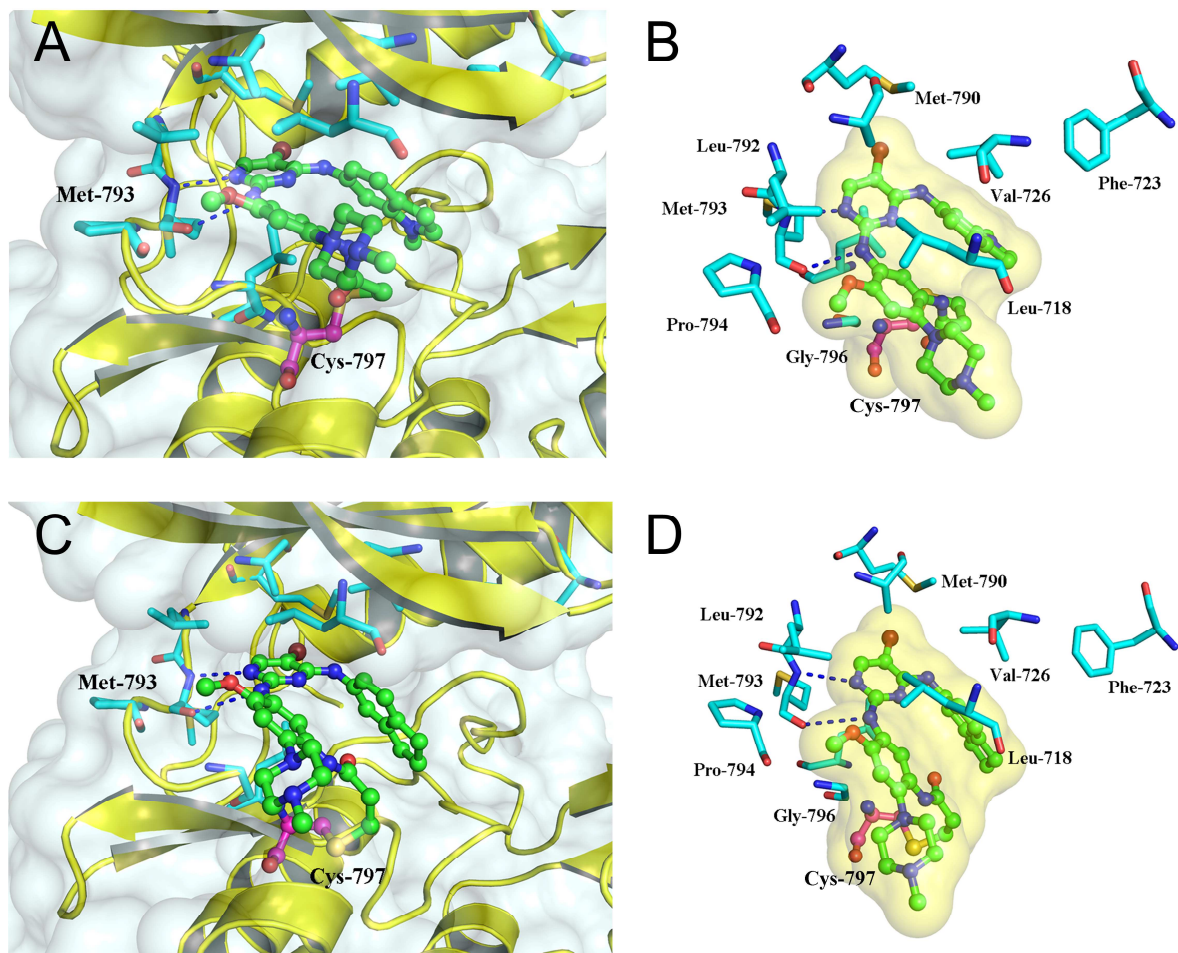
ACCEPTED MANUSCRIPT

**1** (WZ4002)**2** (CO-1686)**3** (AZD9291)**4** (EGF816)**5****6**

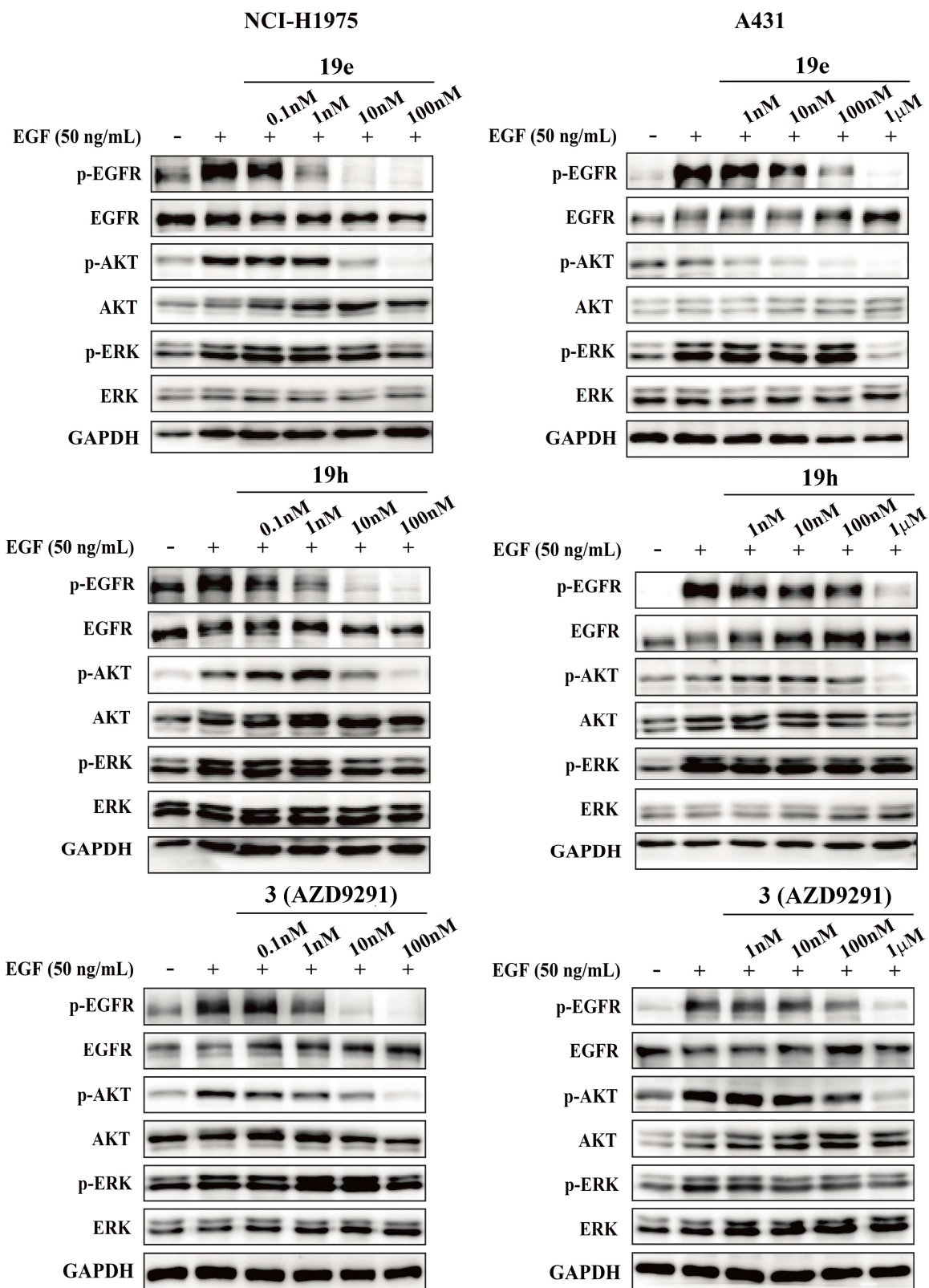


ACCEPTED

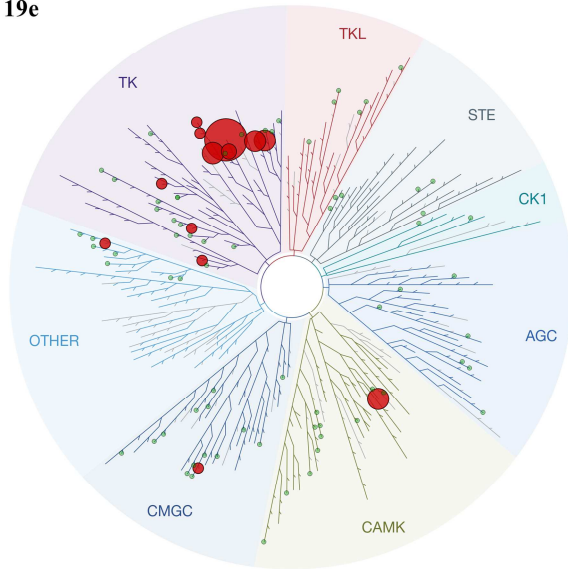






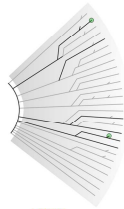


19e

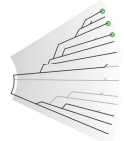


ATYPICAL

MUTANT



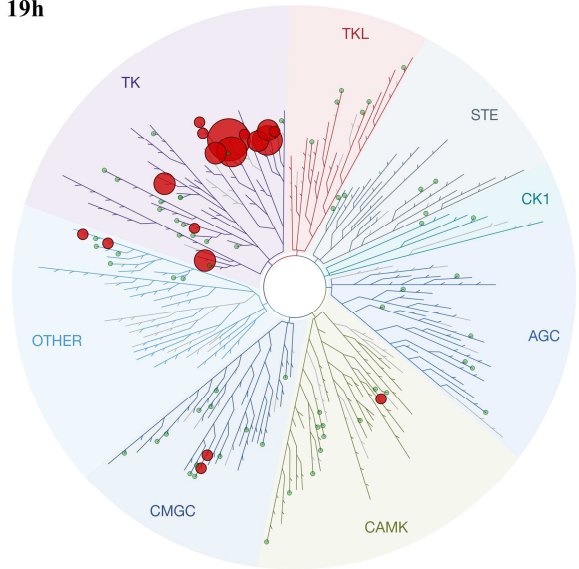
LIPID



PATHOGEN

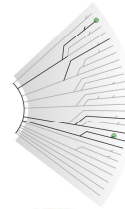


19h

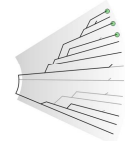


ATYPICAL

MUTANT



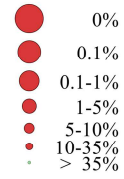
LIPID



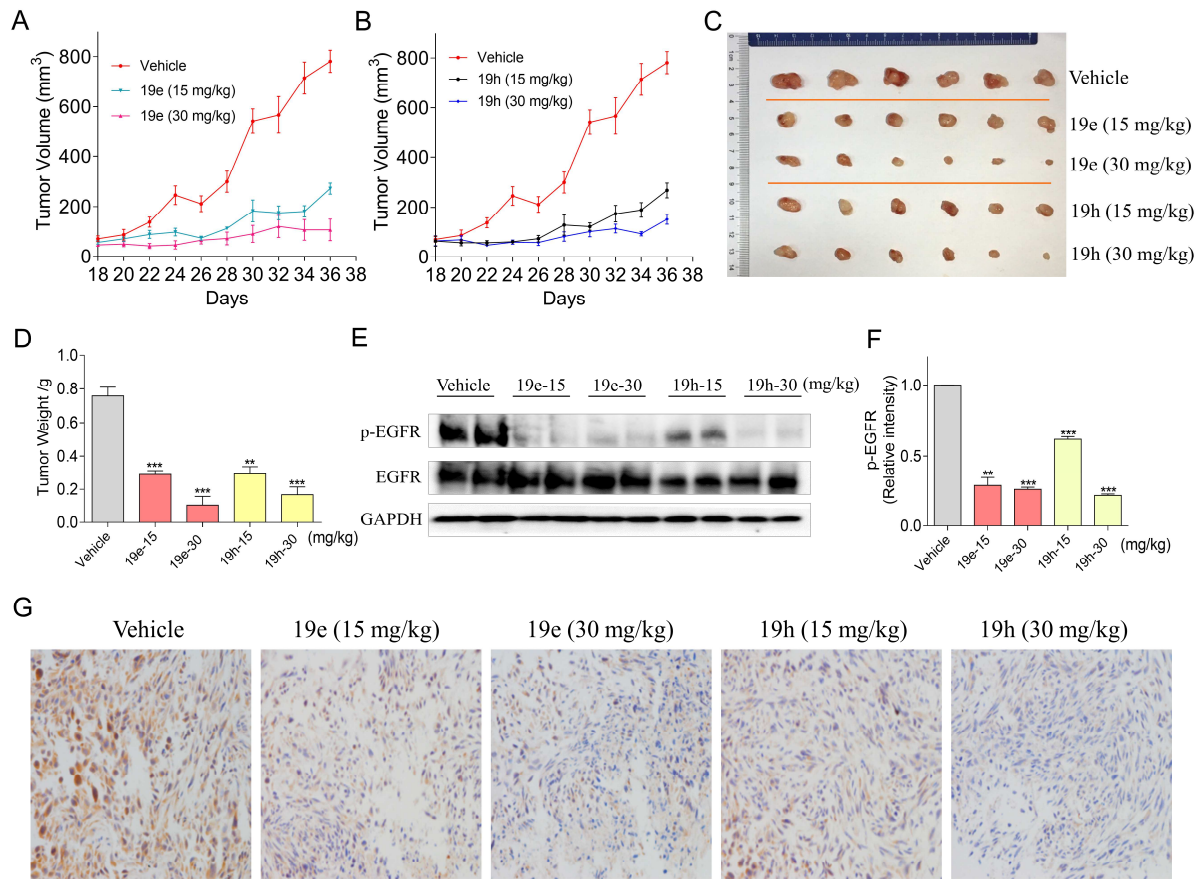
PATHOGEN



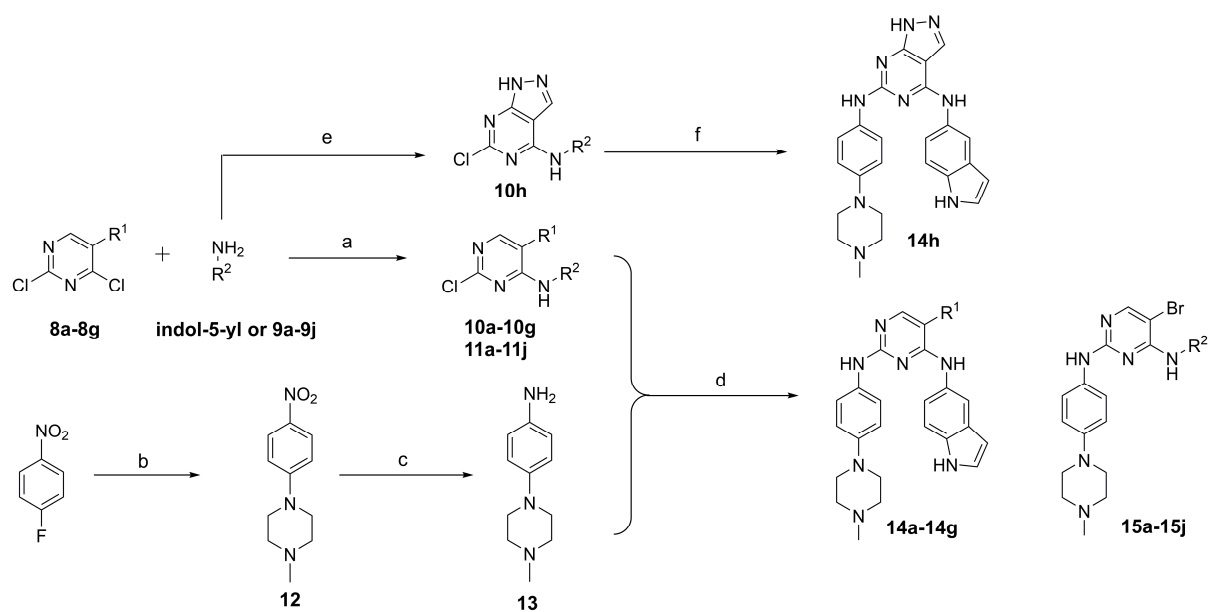
Percent Control



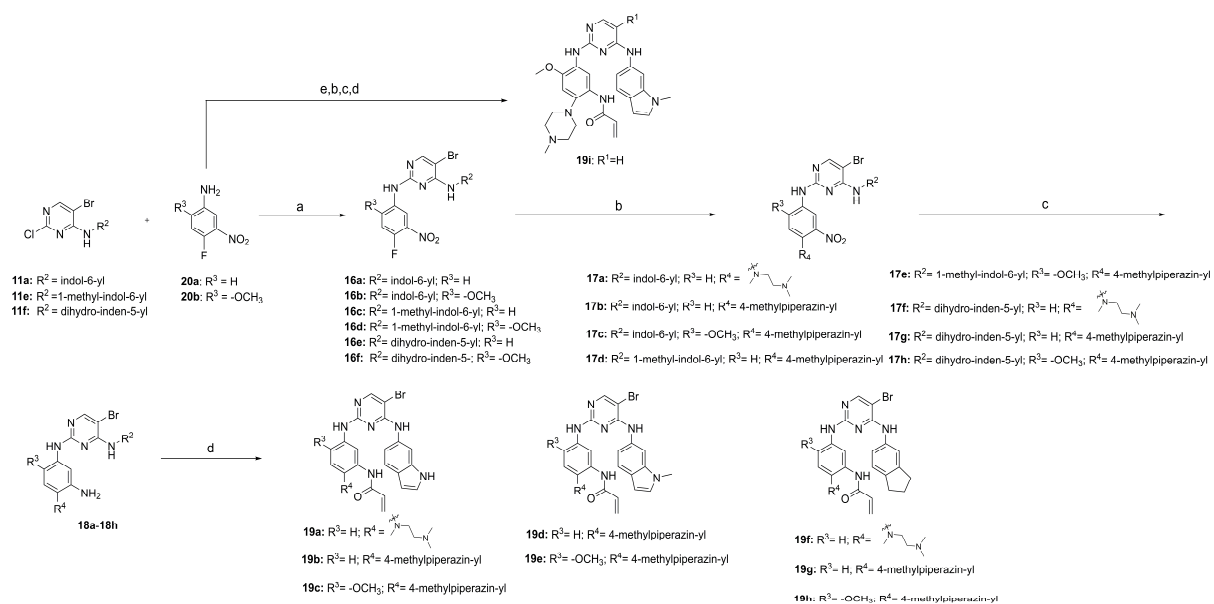
ACCEPTED



Ki67



ACCEPTED MANUSCRIPT



## Highlights:

- Three-step SAR explorations were performed based on the binding mode of lead compound.
- Active compounds showed good pharmacokinetics properties.
- 19e and 19h exhibited great potency and selectivity against EGFR<sup>L858R/T790M</sup> kinase.
- 19e and 19h significantly inhibited tumor growth in H1975 xenograft mouse model.